Low Temperature Physics/Fizika Nizkikh Temperatur, 2021, vol. 47, No. 3, pp. 273–291

Features of kinetic and regulatory processes in biosystems

L. N. Christophorov, V. I. Teslenko, and E. G. Petrov

Bogolyubov Institute for Theoretical Physics of the National Academy of Sciences of Ukraine, Kiev 03680, Ukraine
E-mail: epetrov@bitp.kiev.ua

Received December 07, 2020, published online January 26, 2021

A feature of biological systems is their high structural heterogeneity. This is manifested in the fact that the processes observed at the nanoscopic level are noticeably multistage in time. The paper expounds an approach that allows, basing on the methods of nonequilibrium statistical mechanics, to obtain kinetic equations that enable describing the evolution of slow processes occurring against the background of faster ones. Vibrational relaxation in electronic terms and stochastic deviations of the position of the electronic energy levels of the system from their stationary positions are considered the most important fast processes. As an example, it is shown how the kinetics of one- and two-electron transfer through protein chains, the oxygen-mediated transfer of a triplet excitation in the pigment-protein complex, the kinetics of temperature-independent desensitization of pain receptors, as well as conformational regulation of enzymatic reactions, can be described.

Keywords: density matrix, stochastic field, relaxation, conformation dynamics.

1. Introduction

Biological systems manifest themselves as molecular devices that, on a nanometer scale, perform various types of physicochemical processes, such as enzymatic reactions, conversion of chemical, mechanical, thermal and light energy into each other, synthesis of substances, *etc*. The use of physical mechanisms that control these (and other) processes is one of the most important areas of nanotechnology. The main problem is that, although the basic physical mechanisms governing transitions in condensed matter and small inorganic and organic structures are well understood, the same cannot be said for biosystems. The reason lies in the significant heterogeneity of these systems, which in the same nanoscale volume can contain membranes, globules, chains, ligands, and other fragments. Each of the fragments or a group of fragments, as a rule, is responsible for the performance of its specific functions, including the transfer of energy and charges, conformation transformations, redox reactions, synthesis, *etc*. Heterogeneity leads to a direct or indirect relationships between the structural and functional characteristics of a biosystem. As a result, the characteristic time course of a particular process depends significantly on the indicated relationships. Thus, the system has a hierarchy of characteristic times due to various types of interactions. This hierarchy allows the use of the method of coarse-grained description, which makes it possible to reduce the number of parameters for describing a specific non-equilibrium process. The coarse-grained description method corresponds to Bogolyubov's concept of a hierarchy of relaxation times in both classical and quantum systems [1, 2].

This article shows how the physical processes in biosystems can be described using averaged (coarse-grained) kinetic and dynamic equations. The general approach is illustrated by examples concerning the transport of electrons and excitations, as well as the dynamics of transient conformational processes.

2. Coarse-grained kinetic equations

In statistical mechanics, the average value of the physical quantity O is defined as $\bar{O}(t) = \mathrm{tr}\hat{O}\rho(t)$, where $\hat{O}$ is its operator, and $\rho(t)$ is the nonequilibrium density operator (matrix) of the system [1–4]. The trace (tr) operation assumes summation over all stationary states $|a\rangle$ of the system. The time evolution of the density operator obeys the equation

$$\frac{\partial\rho(t)}{\partial t} = -i\mathcal{L}(t)\rho(t). \qquad (1)$$

Here, $\mathcal{L}(t) = (1/\hbar)[H(t),..]$ is the Liouville superoperator of the system. Note that in Eq. (1) operators are defined by their matrix elements, $\rho_{a'a}(t) = \langle a'|\rho(t)|a\rangle$ and $H_{a'a}(t) = \langle a'|H(t)|a\rangle$, so $\rho(t) = \sum_{aa'}\rho_{a'a}(t)|a'\rangle\langle a|$ and $H(t) = \sum_{aa'}H_{a'a}(t)|a'\rangle\langle a|$. Summation is carried out over

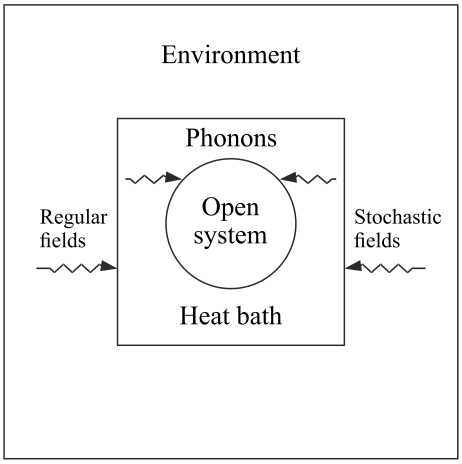

Fig. 1. Scheme shows that the investigated small system is open to the influence of various types of fields, including stochastic ones. The main dissipative and relaxation processes in the system occur due to the exchange of vibrations with the phonon reservoir (heat bath).

all quantum numbers a corresponding to the degrees of freedom of the system under consideration.

As applied to biosystems, it should be noted that despite the complexity of its structural units, the hierarchy of characteristic times of development of each process, as well as its localization in a functional structural unit, makes it possible to physically describe the temporal evolution of the process. For this, a model is considered in which a functional unit of the biosystem is considered as a system with a finite number of "working" degrees of freedom, and the environment is a macroscopic condensed medium with many degrees of freedom. As a result, the processes occurring in the system practically do not change the state of the environment, while the environment can significantly affect the transitions in the system [5–8]. Thus, the system under consideration is an open system in which the temporal behavior of its characteristics is determined by both the internal dynamic processes and contact with the environment, Fig. 1. This contact leads to an exchange of particles and energy, as well as to shifts of energy levels of the system, including stochastic shifts.

The basic equation (1) is applied to the whole structure "system+environment", the Hamiltonian of which $H(t)$ depends on what physical models are used for the system (functional unit of the biosystem) and the environment (surrounding structure or/and solution).

2.1. Markov approximation

In non-magnetic structures, an energy exchange between the system and the environment in most cases occurs through vibration quanta (phonons). This allows us to use the harmonic approximation and thus simulate the environment as a reservoir of phonons with a set of frequencies $\{\omega_\lambda\}$. The establishment of the equilibrium distribution between the vibrational modes occurs in a rather short time $\tau_{vib} \sim 10^{-12}$ s. Therefore, on the time scale $\Delta t \gg \tau_{vib}$, the phonons are in thermodynamic equilibrium and, thus, the environment is considered as the heat bath (B). As a result, the Hamiltonian of the vibrational energy of the environment can be represented in the standard form

$$H_B = \sum_\lambda \hbar\omega_\lambda (b_\lambda^+ b_\lambda + 1/2), \tag{2}$$

where $b_\lambda^+ (b_\lambda)$ is the operator of creation (annihilation) of a phonon of the λth mode. The interaction of the vibrational states of the environment with the vibrational states of the electronic terms of the system leads to the fact that during the characteristic time $\tau_m \sim \tau_{vib}$ the population $P_{mv}(t)$ of the vth vibrational level of the mth electronic term becomes quasi-equilibrium [9]. This means that the ratio between the partial occupancies, $P_{mv}(t)/P_{mv'}(t) = \exp[-\hbar\omega_m(v-v')/k_BT]$, is the time-independent quantity (k_B and T are Boltzmann's constant and absolute temperature, respectively). This means that the population of the vth level $P_{mv}(t) = W_{mv}P_m(t)$ depends only on the equilibrium probability

$$W_{mv} = \exp(-\hbar\omega_m v/k_BT) / \sum\nolimits_v \exp(-\hbar\omega_m v/k_BT),$$

and the integral occupancy of the mth term, $P_m(t) = \sum_v P_{mv}(t)$. The temporal evolution of the latter occurs on the time scale $\Delta t \sim \tau_{tr}$ that strongly exceeds the τ_{vib}. Thus, if the condition

$$\tau_{tr} \gg \tau_{vib} \tag{3}$$

is satisfied, then a coarse-grained description related to the time scale $\Delta t \sim \tau_{tr}$ can be used. This allows us to restrict ourselves to analyzing the temporal behavior of integral state occupancies $P_m(t)$ only. In addition, in this case, harmonic vibrations of the system (intrasystem phonons) are in thermodynamic equilibrium and, therefore, can also be attributed to the phonon reservoir. Accordingly, it is assumed that the vibrational modes with frequencies ω_m belonging to the mth electronic term can be included in the λ-modes of the bath Hamiltonian (4). In other words, the number of the vibrational level $v = 0, 1, 2, \ldots$ in the electronic term exactly corresponds to the number of phonons n_λ of the λth mode associated with the term.

The equilibrium density matrix of the phonon bath has the form

$$\rho_B = e^{-H_B/k_BT} / \mathrm{tr}_B e^{-H_B/k_BT}. \tag{4}$$

The symbol tr_B denotes the summation over all vibration states $n_\lambda = 0, 1, 2, \ldots$, which determine the multimode phonon states $\prod_\lambda |n_\lambda\rangle$ of the heat bath. The average number of phonons with energy $E_\lambda = \hbar\omega_\lambda$ is given by the Bose–Einstein distribution function

$$\bar{n}_\lambda = \mathrm{tr}_B(b_\lambda^+ b_\lambda \rho_B) = [e^{\hbar\omega_\lambda/k_BT} - 1]^{-1}. \tag{5}$$

The total Hamiltonian of the "system+environment" can be represented in the form

$$H(t) = H_0 + \Delta H(t) + H_{SB}, \tag{6}$$

where the time-independent part,

$$H_0 = H_S + H_B, \tag{7}$$

contains the component $H_S = \sum_m E_m |m\rangle\langle m|$ with E_m being the energy of the mth electronic term of the system in an electron-conformation state $|m\rangle$. The second component is the bath Hamiltonian (2), which contains the vibration modes of the environment and the system. The eigenvalues and eigenstates of the H_0 are, respectively, $E_m + \sum_\lambda \hbar\omega_\lambda (n_\lambda + 1/2)$ and $|m\rangle|n_\lambda\rangle$, where $|n_\lambda\rangle = (n_\lambda!)^{-1/2}(b_\lambda^+)^{n_\lambda}|0\rangle$ is the bath state with $n_\lambda = 0, 1, 2, ...$, the number of phonons ($|0\rangle$ denotes the phononless state, that is, the phonon vacuum). The contribution $\Delta H(t)$ is the result of the action of regular or stochastic fields, and H_{SB} is the Hamiltonian of the interaction between the electronic and nuclear degrees of freedoms.

Nucleus displacements have two dynamic effects. The first of them is the polaron shift, which reduces the electronic energy $E_m^{(0)}$ of a system (found in the adiabatic approximation at a certain equilibrium position of the nuclei) to

$$E_m = E_m^{(0)} - \sum_\lambda (g_m^{(\lambda)})^2 \hbar\omega_\lambda. \tag{8}$$

Here, $g_m^{(\lambda)} = \chi_m^{(\lambda)}/\hbar\omega_\lambda$ is the displacement parameter, which is proportional to the constant of "transverse" coupling $\chi_m^{(\lambda)}$ between the system and the environment (such a coupling does not lead to intrasystem transitions but only shifts its energy levels). The second dynamic effect is the formation of the phonon assisted intrasystem transitions accompanied by the creation/annihilation of the phonons. In the systems where transitions occur between *nonadiabatic* terms, the transition operator can be represented as [10, 11]

$$H_{SB} = H_{\text{tr}} = \sum_{m,m'(\neq m)} V_{m'm}\, e^{\sigma_{mm'}} |m'\rangle\langle m|, \tag{9}$$

where $V_{m'm}$ is the electronic transition matrix element. As a rule, the Hamiltonian (9) is used to describe the energy and charge transport in structures containing spaced centers of localization of charges or excitons. The transitions between adiabatic terms are associated with the nonadiabatic operator [12]

$$H_{SB} = H_{\text{nonad}} = \sum_{m,m'(\neq m)} \sum_\lambda \chi_{m'm}^{(\lambda)}\, e^{\sigma_{mm'}} (b_\lambda - b_\lambda^+) |m'\rangle\langle m|, \tag{10}$$

where $\chi_{mm'}^{(\lambda)}$ is the electronic nonadiabatic parameter. Hamiltonian (10) is most often used to describe the intersystem crossing. Both Hamiltonians contain the operator $\sigma_{mm'} = \sum_\lambda g_{mm'}^{(\lambda)}(b_\lambda - b_\lambda^+)$ which depends on the difference $g_{mm'}^{(\lambda)} = g_m^{(\lambda)} - g_{m'}^{(\lambda)}$ in the displacement of nuclei in the electronic states $|m\rangle$ and $|m'\rangle$.

The most complete information on the behavior of the system in time is reflected in the probability of occupation of the mth state of the system (state occupancy), $P_m(t) = \langle m|\rho_s(t)|m\rangle$, where $\rho_s(t) = \text{tr}_B\rho(t)$ is the density matrix of the system, and $\rho(t)$ is the density matrix of the "system+environment", which evolves in accordance with the Liouville equation (1). Assuming H_{SB} as a perturbation, in accordance with the approach based on the nonequilibrium density matrix method [3, 4, 13, 14], we obtain the following integro-differential master equation for the required state populations:

$$\dot{P}_m(t) = -\sum_{m'} \int_0^t d\tau \left[G_{mm'}(\tau)P_m(t-\tau) - G_{m'm}(\tau)P_{m'}(t-\tau)\right]. \tag{11}$$

A time behavior of the kernel

$$G_{mm'}(\tau) = \frac{2}{\hbar^2}\text{Re}[e^{-i\Omega_{mm'}\tau}\Lambda_{mm'}(\tau)F_{mm'}(\tau)] \tag{12}$$

is controlled by the stationary transition frequency $\Omega_{mm'} = (1/\hbar)(E_m - E_{m'})$ as well as the factors $\Lambda_{mm'}(\tau)$ and $F_{mm'}(\tau)$. The form of $\Lambda_{mm'}(\tau)$ is specified by the type of transitions caused by the system-bath interaction H_{SB}. For example, in the case of transitions between nonadiabatic terms we have

$$\Lambda_{mm'}(\tau) = |V_{m'm}|^2 \prod_\lambda \sum_{l_\lambda=-\infty}^{\infty} \Phi_{mm'}^{(\lambda,l_\lambda)} e^{il_\lambda\omega_\lambda\tau}, \tag{13}$$

where quantity

$$\Phi_{mm'}^{(\lambda,l_\lambda)} = e^{-D_{mm'}^{(\lambda)}} I_{|l_\lambda|}\left(z_{mm'}^{(\lambda)}\right)\left[\frac{\bar{n}_\lambda + 1}{\bar{n}_\lambda}\right]^{\frac{l_\lambda}{2}} \tag{14}$$

reflects the contribution of the processes carried out with participation of l_λ phonons. The modified Bessel function $I_{|l|}(z)$ and Debye–Waller factor $D_{mm'}^{(\lambda)} = (g_{mm'}^{(\lambda)})^2(2\bar{n}_\lambda + 1)$ depend on the argument $z_{mm'}^{(\lambda)} = 2(g_{mm'}^{(\lambda)})^2\sqrt{\bar{n}(\bar{n}+1)}$, which is thermally controlled. It is important to note that for $l_\lambda > 0$ the function $\Phi_{mm'}^{(\lambda,l_\lambda)}$ does not disappear at low temperatures. In fact, if $\bar{n}_\lambda \to 0$, then according to the asymptotic of $I_{|l|}(z) \approx (z/2)^{|l|}(1/|l|!)$, which is valid for the Bessel function at $z \ll 1$, we obtain (note $l_\lambda \neq 0$):

$$\Phi_{mm'}^{(\lambda,l_\lambda)} \approx \exp\left[-(g_{mm'}^{(\lambda)})^2\right]\left(g_{mm'}^{(\lambda)}\right)^{2|l_\lambda|}/|l_\lambda|! \times \times\left[(\bar{n}_\lambda + 1)\Theta(l_\lambda) + \bar{n}_\lambda\Theta(-l_\lambda)\right]. \tag{15}$$

If m and m' are the molecular terms with the corresponding vibrational levels, then the relaxation processes responsible for the establishment of the equilibrium distribution

among the vibrational levels of the terms are concentrated in the factor

$$F_{mm'}(\tau) = \mathrm{e}^{-\gamma_{\mathrm{vib}}\tau}, \tag{16}$$

where $\gamma_{\mathrm{vib}} = (\tau_m^{-1} + \tau_{m'}^{-1})$ is the characteristic rate of the vibrational relaxation within the terms m and m' [9]. As $\gamma_{\mathrm{vib}} \sim \tau_{\mathrm{vib}}^{-1}$, the quantity $F_{mm'}(\tau)$ decreases exponentially on the time scale $\Delta\tau \sim \tau_{\mathrm{vib}}$. The characteristic time τ_{vib} is much shorter than the time scale $\Delta t \sim \tau_{\mathrm{tr}}$, on which the temporal evolution of occupancies takes place. Therefore, in Eq. (11), we can extend the upper limit of integration to infinity and neglect the non-markovity setting $P_{m'}(t-\tau) \approx P_{m'}(t)$. This reflects the Markov nature of the transport process, in which the temporal behavior of the integral populations is governed by the balance kinetic equations

$$\dot{P}_m(t) = -\sum_{m'}\left[K_{mm'}P_m(t) - K_{m'm}P_{m'}(t)\right]. \tag{17}$$

The corresponding transition rate constants have the form

$$K_{mm'} = \int_0^\infty d\tau G_{mm'}(\tau), \tag{18}$$

where the integrand is determined by the Eq. (12).

If the transition occurs between the non-adiabatic electronic terms, then using Eqs. (13) and (14) gives

$$K_{mm'} = \frac{2\pi}{\hbar}|V_{m'm}|^2\,(FC)_{mm'}. \tag{19}$$

The effect of phonons on the transition efficiency is concentrated in the Franck–Condon factor [14–16], which reads

$$(FC)_{mm'} = \frac{1}{\hbar}\prod_\lambda \sum_{l_\lambda=-\infty}^{\infty} \Phi_{mm'}^{(\lambda,l_\lambda)}\,\delta\left(\Omega_{mm'} - \sum_\lambda l_\lambda\omega_\lambda\right). \tag{20}$$

In (20), the form of the FC factor is represented in the most frequently used version when Lorentzian $L(\Omega) = (1/\pi)[\gamma/(\Omega^2+\gamma^2)]$ is replaced by delta-function $\delta(\Omega)$. This simplification is due to the fact that the summation over l_λ in the interval $[-\infty,+\infty]$ may be replaced by the integration over the same infinite interval.

2.2. Stochastic influence

In addition to the dynamic effects, one should also take into account the stochastic effect of the environment on the system. The stochastic movements of the structural groups of the environment create time-dependent random fields [8, 11, 17–21], which can be caused by fluctuations of the energy of separate environmental groups [22]. These random fields affect the system in such a way that its energy levels E_m experience stochastic displacements $\Delta E(t)$. Consequently, the Hamiltonian H_S of the system acquires stochastic addition $\Delta H(t) = \sum_m \Delta E_m(t)\,|m\rangle\langle m|$, which is the time-dependent contribution to the overall Hamiltonian (7). In the model under consideration, the fluctuations in the environment lead to a stochastic change in the number of phonons of each of the λth mode. Therefore, the mean vibration energy of the bath, $\bar{E}$, and the corresponding mean square energy fluctuation, $\overline{\delta E^2} = \overline{(E-\bar{E})^2} = k_B T^2(\partial\bar{E}/\partial T)$ [23], read

$$\bar{E} = \sum_\lambda \bar{E}_\lambda, \quad \bar{E}_\lambda = \hbar\omega_\lambda(\bar{n}_\lambda + 1/2), \tag{21}$$

and

$$\overline{\delta E^2} = \sum_\lambda \overline{\delta E_\lambda^2}, \quad \overline{\delta E_\lambda^2} = (\hbar\omega_\lambda)^2[\bar{n}_\lambda(\bar{n}_\lambda+1)], \tag{22}$$

respectively. If we take into account that during vibrations of the structural groups of the environment, a part of the vibrational energy is transferred to the system, then the position of energy levels of the system becomes stochastic, $E_m(t) = E_m + \Delta E_m(t)$. As a result, instead of regular factor $F_{mm'}(\tau)$, a stochastic factor $\mathcal{F}_{mm'}(\tau) = -i\int_0^\tau d\tau'\Delta\Omega_{mm'}(\tau')$ appears, which is a functional of the stochastic value $\Delta\Omega_{mm'}(\tau) = [(\Delta E_m(\tau) - \Delta E_{m'}(\tau))]/\hbar$. As a result, the integral occupancies are also stochastic occupancies $\mathcal{P}(m,t)$. Now, to find the kinetic master equation for the observed occupancies $P_m(t)$, the original Liouville equation (1) must be averaged over the realizations of the random variable $\Delta E_{mm'}(\tau)$.

In biosystems, a situation is often realized when transient processes occur at characteristic times τ_{tr}, which significantly exceed not only the characteristic times τ_{vib} of the establishment of equilibrium vibrations, but also the characteristic times τ_{stoch} of stochastic changes associated with the movement of structure units of the environment. In particular, stochastic shifts occur over a wide range of characteristic times τ_{stoch} of the order of 10^{-8}–10^{-10} s [24, 25]. In this case, a coarse-grained description of the kinetics becomes possible. As shown in Fig. 2, the behavior of the population $\mathcal{P}(m,t)$ on the time-scale $\Delta t \sim \tau_{\mathrm{stoch}}$ is random, while on the time-scale $\Delta t \sim \tau_{\mathrm{tr}}$ its average value $P_m(t)$ reflects smoothed evolution over time. In our case,

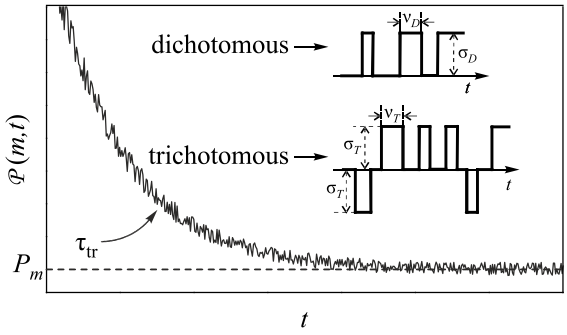

Fig. 2. Random deviations of the population $\mathcal{P}(m,t)$ of the mth state of the system from its average value $P_m(t) = \langle\langle\mathcal{P}(m,t)\rangle\rangle$ is due to the action of stochastic fields (discrete dichotomous and trichotomous deviations are shown). If condition (23) is satisfied, a smoothed (coarse-grained) description can be carried out on the time scale $\Delta t \sim \tau_{\mathrm{tr}}$.

the time τ_{tr} is related to the transition rates caused by system-bath interaction H_{SB}, and, thus, the time $\Delta t \sim \tau_{stoch}$ characterizes stochastic variations of the factor $\mathcal{F}_{mm'}(\tau)$. Therefore, according to the averaging procedure [8, 11, 17, 21, 22, 26] and by virtue of the condition

$$\tau_{tr} \gg \tau_{stoch} \tag{23}$$

we again come to equations (11) and (12), where now $P_m(t) = \langle\langle \mathcal{P}(m,t)\rangle\rangle$, $P_{m'}(t-\tau) = \langle\langle \mathcal{P}(m',t-\tau)\rangle\rangle$ and

$$F_{mm'}(\tau) = -i\langle\langle \int_0^\tau d\tau' \Delta\Omega_{mm'}(\tau')\rangle\rangle \tag{24}$$

are the averaged quantities.

The basic principles of averaging stochastic functionals [27–31] indicates that to calculate the $F_{mm'}(\tau)$, it is necessary to know the mean amplitudes σ_j of $\Omega_{mm'}(\tau)$ realizations and the stationary probabilities w_j of these realizations. In the important special case of the dichotomous random process, the quantity $\Omega_{mm'}(\tau)$ has only two realizations, σ_1 and σ_2, which are executed with probabilities $w_1 = \nu_2/(\nu_1+\nu_2)$ and $w_2 = \nu_1/(\nu_1+\nu_2)$, respectively. Then, following the exact results [8, 26], we obtain

$$F_{mm'}(\tau) = \frac{s_+ e^{s_-\tau} - s_- e^{s_+\tau}}{s_+ - s_-} e^{-i\Omega^{(av)}\tau}, \tag{25}$$

where $\Omega^{(av)} = w_1\sigma_1 + w_2\sigma_2$ is the average value of the $\Omega_{mm'}(\tau)$. The main temporal behavior of the factor $F_{mm'}(\tau)$ is specified by the quantities

$$s_\pm = -(1/2)\left[\nu_c \pm r\cos\phi - i(\Delta w\Delta\sigma \pm r\sin\phi)\right], \tag{26}$$

where $\nu_c = (\nu_1+\nu_2)/2$, $\Delta\sigma = \sigma_1 - \sigma_2$, $\Delta w = w_1 - w_2$, $r = \sqrt{(\nu_c^2 - \Delta\sigma^2)^2 + 4(\Delta w\Delta\sigma)^2}$, and $\tan(2\phi) = 2\Delta w\Delta\sigma/(\nu_c^2 - \Delta\sigma^2)$.

A fundamentally important role of the stochastic shift of the energy levels of the system lies in the generation of the damping factors $\gamma_{stoch} = (1/2)(\nu_c \pm r\cos\phi)$, contained in the quantities s_+ and s_-. The presence of exponential decay on the time scale $\Delta\tau \sim \tau_{stoch} = \gamma_{stoch}^{-1}$ shows that if the kinetic process is described by Eq. (11) and develops on a time scale $\Delta t \sim \tau_{tr}$ satisfying inequality (23), then we can set $P(m',t-\tau) \approx P_{m'}(t)$ and, as in the case of fast vibrational relaxation, the upper limit of integration can be extended to infinity. Thus, as a result of averaging, we come again to the balance-like kinetic equations (17). In these equations, the average rates of the $m \to m'$ transition in a system interacting with a stochastic environment have the form (19) where, however, the integrand $G_{mm'}(\tau)$, Eq. (12), contains the stochastically averaged factor (24). In the case of a dichotomous fluctuations, the latter is given by the Eq. (25).

2.3. Thermodynamic fluctuations

Specific reasons for the formation of the amplitudes σ_j of the stochastic variable $\Delta\Omega_{mm'}(\tau) = \Delta E_{mm'}(\tau)/\hbar$ can be different. If the deviation of the environment energy is explained by the deviation of vibrational quanta from their mean values $\bar{n}_\lambda$, then it can be assumed that the environment is in thermodynamic equilibrium and the vibrations of its structural groups are close to harmonic. Therefore, the stochastic addition δE_m to the energy E_m can be caused by the fluctuation shift $\sum_\lambda \hbar\omega_\lambda \delta n_\lambda$ in the vibrational energy of the environment. Since energy is conserved in each act of energy exchange between the environment (phonon reservoir) and the system, the condition

$$E_m + \delta E_m + \sum_\lambda \hbar\omega_\lambda (n_\lambda + \delta n_\lambda) =$$

$$= E_{m'} + \delta E_{m'} + \sum_\lambda \hbar\omega_\lambda (n'_\lambda + \delta n'_\lambda) \tag{27}$$

is satisfied even in the presence of random deviations of $\delta n_\lambda = n_\lambda - \bar{n}_\lambda$ and $\delta n'_\lambda = n'_\lambda - \overline{n'_\lambda}$. The phonon assisted transition $m \to m'$ occurs at a fixed energy difference $E_m - E_{m'} = \sum_\lambda \hbar\omega_\lambda (n'_\lambda - n_\lambda)$. Hence, according to the Eq. (27), realization of the random energy deviations $\Delta E_{mm'}(\tau)$ occurs via stochastic values $\delta E_{mm'} = \delta E_m - \delta E_{m'} = \sum_\lambda \hbar\omega_\lambda (\delta n'_\lambda - \delta n_\lambda)$. For noninteracting phonons, the averaging gives $\overline{\delta n'_\lambda} = \overline{\delta n_\lambda} = 0$ and $\overline{\delta n'_\lambda \delta n_\lambda} \simeq \overline{\delta n_\lambda^2}\delta_{n'_\lambda, n_\lambda}$. Then according to the Eqs. (21) and (22) we get

$$\overline{\delta E}_{mm'} = \sum_\lambda \overline{\delta E}_\lambda = 0,$$

$$\overline{(\delta E_{mm'})^2} = 2\sum_\lambda \overline{\delta E_\lambda^2}. \tag{28}$$

The expressions (28) show that the average thermodynamic fluctuations depend on the number of oscillator modes λ involved in the contact with the system. If the mean stochastic life-time $\tau_{stoch}^{(\lambda)}$ of realization of each quantity δE_λ (and thus δE_λ^2) is approximately the same, then with a large number of oscillators the stochastic influence of the environment on the $m \to m'$ transitions should manifest itself in the form of white noise, while with a finite number of oscillators the stochastic effect will be discrete.

In biosystems, discrete fluctuations are of particular importance, since they relate to well-defined structural units of the system. For example, the study of protein fluorescence has showed that the stochastic behavior of the fluorescence intensity reflects the fluctuation dynamics of proteins, and this dynamics is rather well manifested in the form of a dichotomous process covering the nanosecond and microsecond regions [32]. Therefore, we will consider the role of such dichotomous fluctuations assuming that among the possible oscillatory modes λ, the most effective is mode λ_* of frequency ω_*, which leads to fluctuations of the value $(E_m - E_{m'})/\hbar = \Omega_{mm'}$. Hence, according to the results presented in the Eq. (28), we have $\overline{\delta E}_{mm'} = \overline{\delta E_*}$ and $(\delta E_{mm'})^2 = 2\delta E_*^2$. In classical physics, the linear frequency $\nu = \omega/2\pi$ corresponds to the frequency of collision of

a particle with the walls of the potential well. The collision results in an exchange of energy between the oscillator and the system. In the quantum case, assuming that at each collision with the wall the quantum of vibrational energy is acquired by a system or the oscillator receives a quantum of energy from the system (one-phonon approximation), we can relate $\nu_* = \kappa\bar{\omega}_* / 2\pi = (\kappa / 2\pi\hbar)\bar{E}_*$ to the frequency of realization of the one-phonon fluctuations (the temperature-independent parameter $\kappa < 1$ characterizes the efficiency of energy exchange between the system and the phonon reservoir). Positive and negative mean amplitudes of this fluctuation are $\sigma_\pm = \pm\sigma_*$ where $\sigma_* = [2\delta E_*^2]^{1/2} / \hbar$. Hence, the simplest case of thermodinamic fluctuations of the vibrational energy of the environment leads to dichotomous stochastic displacements in the transition frequency $\Delta\Omega_{mm'}$ of the dynamic system. The frequency ν_* and the amplitude σ_* of these symmetric displacements are determined as (see also Refs. 11, 21)

$$\nu_* = \kappa(\omega_* / 4\pi)(2\bar{n}_* + 1),$$
$$\sigma_* = \omega_*\sqrt{2\bar{n}_*(1+\bar{n}_*)}. \quad (29)$$

To be consistent with a standard symmetric dichotomous process, the escape frequencies and the amplitudes of the random deviations must be $\nu_1 = \nu_2 = \nu_c \equiv \nu_*$ and $\sigma_1 = -\sigma_2 \equiv \sigma_*$, respectively. Then, based on the exact results, Eqs. (25) and (26), we obtain $\Omega_{av} = \langle\langle\Delta\Omega_{mm'}(\tau)\rangle\rangle = 0$ and $s_{1,2} = -(1/2)[\nu_* \pm \sqrt{\nu_*^2 - 4\sigma_*^2}]$.

When the classical limit ($\bar{n}_* \gg 1$) is satisfied, then

$$F_{mm'}(\tau) = e^{-\gamma_{stoch}\tau}\cos\sigma_*\tau,$$
$$\gamma_{stoch} \simeq \kappa(k_B T / 4\pi\hbar). \quad (30)$$

At the low temperature limit ($\bar{n}_* \ll (\kappa^2 / 8\pi^2) \ll 1$) we get

$$F_{mm'}(\tau) = e^{-\gamma_{stoch}\tau},$$
$$\gamma_{stoch} \simeq (8\pi\omega_* / \kappa)e^{-\hbar\omega_*/k_B T}. \quad (31)$$

Averaged kinetic equations (20) with the transition rates determined by the Eqs. (19), (12)–(14), and (24) are used below as a basis for a coarse-grained description of kinetic processes on a time scale $\Delta t \sim \tau_{tr}$ [cf. condition (23)].

3. Results and discussion

This section shows how the above approach to describing the time behavior of the populations of the states of an open system is used to analyze kinetic and dynamic processes in various types of biosystems. To do this, in each specific case, a model is used that defines the states involved in the transitions and the interactions responsible for the transitions. As follows from Eqs. (12) and (19), the features of the temporal evolution of the state occupancies of the system are determined by the factors $\Lambda_{mm'}$ and $F_{mm'}$, which reflect the interactions between the electronic and nuclear degrees of freedom.

3.1. Single-electron transfer through protein chains

There are many different types of charge transfer processes responsible for redox reactions in biosystems. Among them, a special place is occupied by reactions of one- and two-electron transfer between spaced redox centers. In many cases, such reactions are mediated by bridging structures (B) that connect the donor (D) and acceptor (A) centers. The role of D and A centers is attributed to the redox groups, while the D–A connection is often carried out through protein chains [33–35] or DNA [36, 37]. To understand the physical mechanism of the formation of electron transfer between spaced redox centers, in the late 70s, a donor-acceptor model of electron transfer through a protein chain was proposed, where the peptide groups of the protein chain played the role of a bridge for electron transfer [38–41]. The model made it possible to explain the exponential drop in donor-acceptor electron transfer rate k_{DA} with an increase in the number of repeating bridge units N. This indicates the presence of a superexchange interaction between redox centers and, thus, explains the long-range electron tunneling through the protein structure. Further improvement of the superexchange model allowed one to find the conditions for its applicability for various molecular DBA systems [42–46] and to show that in the limiting cases the modified superexchange model covers the limiting case of deep tunneling and mimics tunneling through a rectangular barrier, thus making it possible to determine the effective mass of a tunneling electron, as well as the height and length of the barrier [39, 47]. If the energy gap between the highest energies of the donor and the lowest energy of bridging groups allows the temperature activated transfer of an electron from the donor to the bridge, the transfer process in the DBA system becomes noticeably more complicated. This is reflected in the mixing of the superexchange and hopping transfer mechanisms [40, 41, 48–50]. In the case of nonadiabatic D–A electron transport, the kinetics is described by the system of equations (17) with the hopping rates (19). The electronic states of the DBA system $|m\rangle$ are characterized by the presence of a transferred electron on their structure units, i.e., $m = D, A, B_1, B_2, ..., B_N$ where $D \equiv D^-BA$, $A \equiv DBA^-$, $B_m \equiv DB_m^-A$ (symbols $B \equiv B_1B_2...B_N$ and $B_m \equiv B_1B_2...B_m^-...B_N$ denote a bridge chain without an extra electron and with the transferred electron located on the mth bridge unit, respectively). The normalization condition under which the system of $N + 2$ kinetic equations (17) is solved has the form

$$P_D(t) + P_B(t) + P_A(t) = 1. \quad (32)$$

Therefore, if the integral population of the bridging units by the transferred electron is insignificant, i.e.,

$$P_B(t) = \sum_{m=1}^{N} P_m(t) \ll 1, \quad (33)$$

and, therefore,

$$P_D(t) + P_A(t) \simeq 1, \tag{34}$$

then an electron transfer in the DBA system looks like a oxidation-reduction reaction only between D and A centers. In this case, the N bridging states $|B_m\rangle$ with energies E_m play a virtual role in electron transfer. The condition (33) is fundamentally important when obtaining analytical expressions for the bridge mediated electron-transfer rates [40, 49, 50]. One can show [41] how the $(N+1)$-exponential kinetics reduces to one-exponential kinetics, describing the time evolution only for $P_D(t)$ and $P_A(t)$. Such a reduction corresponds to a coarse-grained description of the of D–A electron transfer, which is characterized by the forward and backward D–A rates, k_{DA} and k_{AD}, respectively (Fig. 3). Within the framework of a coarse-grained description, we get

$$P_D(t) \simeq \frac{1}{k_{ET}}[k_b + k_f e^{-k_{ET}t}],$$

$$P_A(t) \simeq \frac{k_f}{k_{ET}}[1 - e^{-k_{ET}t}], \tag{35}$$

where the overall transfer rate

$$k_{ET} = k_f + k_b, \tag{36}$$

determines the time-scale $\Delta t \sim \tau_{tr} = k_{ET}^{-1}$ of the electron-transfer process.The forward rate

$$k_f = k_f^{(hop)} + k_f^{(sup)} \tag{37}$$

(and the backward rate $k_b = k_f e^{-(E_A - E_B)/k_B T}$) contains two contributions. One of them,

$$k_f^{(hop)} = \left(\frac{k_{-1}k_2}{k_1 + k_2}\right)\frac{1}{1 + \xi(N-1)}, \tag{38}$$

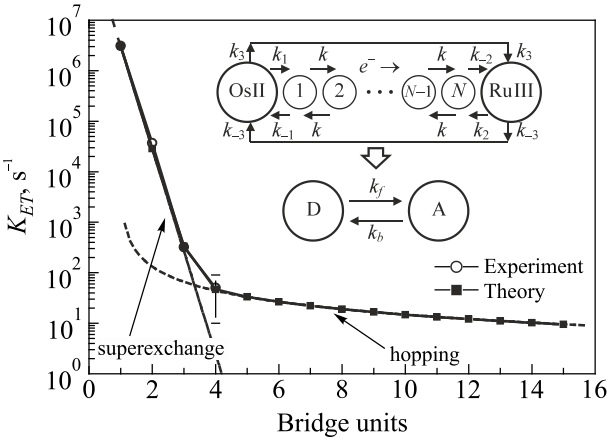

Fig. 3. The dependence of the overall rate K_{ET} of electron transfer from OsII n-donor to RuIII-acceptor (adapted from [41]) occurs according to a mixed mechanism, including direct tunneling (rates k_3 and k_{-3}) and sequential hoppings with the participation of N units of the bridge B (proline chain). For the considered DBA system, the probability of finding a transported electron on the bridge is insignificant and therefore the process is characterized by direct one-step jumps with rates k_f and k_b. Details in the text.

contain the parameter

$$\xi = \frac{k_1 k_2}{k(k_1 + k_2)}, \tag{39}$$

which characterizes the decrease in the electron transfer along the sequential pathway $D \to B_1 \to B_2 \to ... \to B_N \to A$ carried out using the hopping rates $k_1 = k_{1D}$, $k_{-1} = k_{D1}$, $k_2 = k_{NA}$, $k_{-2} = k_{AN}$, and $k = k_{mm\pm1}$, $(m = 1, 2, ..., N)$, (Fig. 3). The form of these rates is given by the Eq. (19).

The second contribution,

$$k_f^{(sup)} = k_3 = k_{0f}^{(sup)} e^{-\zeta(N-1)} \tag{40}$$

reflects the direct $D \to A$ pathway associated with a one-step hopping of an electron between the D and A centers. The parameter

$$\zeta = -2\ln\left(\frac{|V_B|}{\Delta E_D \Delta E_B}\right) \tag{41}$$

characterizes the decrease in the contribution associated with the superexchange D–A coupling. In the Eq. (41), $V_B \equiv V_{mm\pm1}$ is the electron coupling between the nearest bridge units, and $\Delta E_{D(A)} = E_B - E_{D(A)}$ is the energy gap between the bottoms of electronic terms related to the bridge unit and the D(A) center. Figure 3 shows a good correspondence of the theory with experimental results on electron transfer from D(OsII) to A(RuIII) through a biopolymer composed of proline units.

3.2. Two-electron bridge-mediated transfer

Two-electron transport (TET) is a basic physical process that is responsible for redox reactions catalyzed by metalloenzymes. In most cases, TET is accompanied by the capture or release of one or more protons. For example, a hydride ($:H^-$) transport is accompanied by the correlated transport of two electrons and a proton. One of the fundamental problems of multielectron transport is the elucidation of the mechanisms of correlated delivery of electrons from donor to acceptor groups during sequential and concert electron transfer [51]. Following the approach presented in [52], as well as the above results concerning a coarse-grained description of one-electron transfer, we will show how both mechanisms can be realized in a nanomolecular complex, where the transfer of two electrons from a donor to an acceptor occurs with the participation of a bridge structure. The results of the theory are used to explain the experimental data on the reduction of mycothione reductase (MycR) with the oxidizing agent nicotinamide adenine dinucleotide phosphate (NADP).

A model is used where the donor and acceptor centers can have one or two extra electrons, while the bridge has only one. This is possible if the D and A centers have polar groups, and the bridging units are in a hydrophobic environment (this situation is quite typical for a biosystem). As a result, two-electron transfer can be realized using two repeating one-electron routes. During the first route, one of

the two extra electrons occupying the D center is transferred to the A center along the sequential pathway $D^{2-}BA \to D^{-}B_1^{-}A \to D^{-}B_2^{-}A \to ... \to D^{-}B_N^{-}A \to D^{-}BA^{-}$ with forward (k_{D1}, α, k_{NI}) and backward (k_{1D}, β, k_{IN}) rates as well as a one-step (superexchange) pathway $D^{2-}BA \to D^{-}BA^{-}$ with forward (k_{DI}) and backward (k_{ID}) rates. The first route forms an intermediate charging structure $I \equiv D^{-}BA^{-}$, which switch on the second one-electron route. The latter includes the sequential pathway $D^{-}BA^{-} \to DB_1^{-}A^{-} \to DB_2^{-}A^{-} \to ...$ $... \to DB_N^{-}A^{-} \to DBA^{2-}$ with forward (k_{I1}, α, k_{NA}) and backward (k_{1I}, β, k_{AN}) rates as well as a one-step (superexchange) pathway $D^{-}BA^{-} \to DBA^{2-}$ with forward (k_{IA}) and backward (k_{AI}) rates. Schemes of both routes are shown in Fig. 4(a), the rates $k_{mm'}$ are determined by the Eq. (19), (more detail form of the rates is given in Ref. 52).

When the bridge states act as an intermediate and thus the condition (33) is satisfied, then the $D(D^{2-}BA) \to$ $\to I(D^{-}BA^{-})$ and $I(D^{-}BA^{-}) \to A(DBA^{2-})$ transitions related to the routs $j = 1$ and $j = 2$, respectively, are controlled by route rates [Fig. 4(b)]

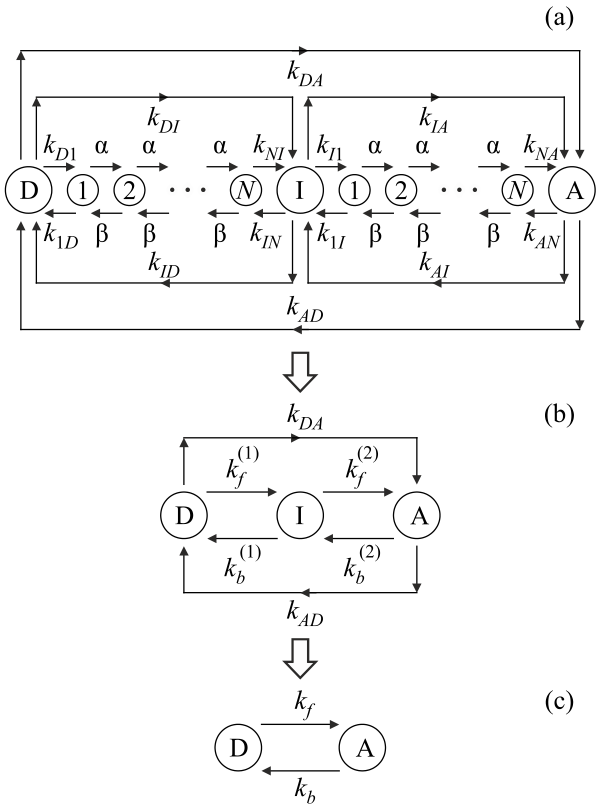

Fig. 4. Scheme (adapted from [52]) of the tunneling and sequential pathways of two electrons from the donor to the acceptor through the bridge with the formation of an intermediate state I (only one of the two electrons was transferred). If the probability of populating the bridge with transferred electrons is small, then, as in the case of one-electron transfer, a coarse-grained description of the process can be made using the rates k_f and k_b. Now these rates contain contributions from the "concert" (two-electron coherent) and sequential transport mechanisms.

$$k_f^{(j)} = \frac{k_{j0}^{(f,\mathrm{seq})}}{1 + \xi_j \dfrac{1 - r^{N-1}}{1 - r}} + k_{j0}^{(f,\mathrm{sup})} \mathrm{e}^{-\zeta_j (N-1)},$$

$$k_b^{(j)} = k_f^{(j)} \mathrm{e}^{-\Delta E_j / k_B T}, \ (r = \beta / \alpha). \qquad (42)$$

They include the contributions caused by the one-electron sequential and superexchange mechanisms of an electron transfer. Corresponding dependence on the number of repeating bridge units is characterized by the quantities

$$\xi_j = \frac{k_{1D}^{(j)} \left(k_{NA}^{(j)} - \alpha(1-r) \right)}{\alpha \left(k_{NA}^{(j)} + k_{1D}^{(j)} \right)} \qquad (43)$$

and

$$\zeta_j = -2 \ln \left[\frac{|V_B|}{\left(\Delta E_D^{(j)} \Delta E_A^{(j)} \right)^{1/2}} \right], \qquad (44)$$

where the factors

$$k_{j0}^{(f,\mathrm{seq})} = \frac{k_{D1}^{(j)} k_{NA}^{(j)}}{k_{NA}^{(j)} + k_{1D}^{(j)}},$$

$$k_{D1(NA)}^{(j)} = \frac{2\pi}{\hbar} |V_{1D(AN)}^{(j)}|^2 \, FC_{1D^{(j)}(A^{(j)}N)}, \qquad (45)$$

and

$$k_{j0}^{(f,\mathrm{sup})} = \frac{2\pi}{\hbar} \frac{|V_{1D}^{(j)} V_{AN}^{(j)}|^2}{\Delta E_D^{(j)} \Delta E_A^{(j)}} FC_{D^{(j)}A^{(j)}} \qquad (46)$$

are respectively the hopping and superexchange one-electron transfer rates for the bridge with a single bridging unit ($N = 1$). In Eqs. (43)–(46) the gaps

$$\Delta E_D^{(1)} = E(D^{-}B^{-}A) - E(D^{2-}BA),$$

$$\Delta E_A^{(1)} = E(D^{-}B^{-}A) - E(D^{-}BA^{-})$$

and

$$\Delta E_D(2) = E(DB^{-}A^{-}) - E(D^{-}BA^{-}),$$

$$\Delta E_A(2) = E(DB^{-}A^{-}) - E(DBA^{2-})$$

specify the energy distances between the electronic working states of the entire DBA system,

The route rates determine the coarse-grained kinetics on the time scale $\Delta t \sim \tau_{DIA} \sim K_1^{-1}, K_2^{-1}$. The overall TET rates

$$K_{1,2} = \frac{1}{2}(c_1 + d_1 \pm \sqrt{(c_1 - d_1)^2 + 4 c_2 d_2}), \qquad (47)$$

where

$$c_1 \equiv k_f^{(2)} + k_b^{(2)} + k_{AD}, \quad c_2 \equiv k_{DA} - k_f^{(2)},$$

$$d_1 \equiv k_f^{(1)} + k_b^{(1)} + k_{DA}, \quad d_2 \equiv k_{AD} - k_b^{(1)}, \qquad (48)$$

determine the kinetic process covering the three states $|j\rangle$, (j = D, I, A), whose integral occupancies are related by the normalization condition

$$P_D(t) + P_I(t) + P_A(t) = 1. \qquad (49)$$

The corresponding scheme of kinetic processes is shown in Fig. 4(b). These processes reflect the two-exponential temporal evolution of the integral occupancies

$$P_j(t) = P_j + C_j^{(1)}\mathrm{e}^{-K_1 t} + C_j^{(2)}\mathrm{e}^{-K_2 t} \tag{50}$$

to their stationary values

$$P_D = (c_1 k_b^{(1)} + d_2 k_f^{(2)})/(c_1 d_1 - c_2 d_2),$$

$$P_A = (c_2 k_b^{(1)} + d_1 k_f^{(2)})/(c_1 d_1 - c_2 d_2) \tag{51}$$

and $P_I = 1 - P_D - P_A$. With a weak population of the intermediate state (i.e. at $P_I(t) \ll 1$), which happens if $k_f^{(1)}, k_b^{(2)} \ll k_f^{(2)}, k_b^{(1)}$, the transfer of two electrons from the D center to the A center manifests itself as a one-exponential kinetic process corresponding to the scheme shown in Fig. 4(c).The temporal behavior of the two-electron occupancies,

$$P_D(t) \simeq \frac{1}{k_{TET}}[k_b + k_f \mathrm{e}^{-k_{TET}t}],$$

$$P_A(t) \simeq \frac{k_f}{k_{TET}}[1 - \mathrm{e}^{-k_{TET}t}], \tag{52}$$

reflects a coarse-grained description on the time-scale $\Delta t \sim \tau_{TET} = k_{TET}^{-1}$ where $k_{TET} = k_f + k_b$ is the overall rate characterizing the two-electron transfer between D and A centers [cf. Fig. 4(c)]. Since $k_{f(b)} = k_{f(b)}^{(\mathrm{step})} + k_{DA(AD)}$, then

$$k_{TET} = k_{TET}^{(\mathrm{step})} + k_{TET}^{(\mathrm{conc})} \tag{53}$$

The component

$$k_{TET}^{(\mathrm{step})} = k_f^{(\mathrm{step})} + k_b^{(\mathrm{step})},$$

$$k_{f(b)}^{(\mathrm{step})} = \frac{k_{f(b)}^{(1)} k_{f(b)}^{(2)}}{k_b^{(1)} + k_f^{(2)}}, \tag{54}$$

is originated by the stepwise mechanism where the partial overall rates are determined by Eq. (42). Physically, these rates are identical to the one-electron transfer rate (37). The component

$$k_{TET}^{(\mathrm{conc})} = k_{DA} + k_{AD} \tag{55}$$

of the overall rate is associated with the concerted mechanism of a two-electron transfer [cf. Figs. 4(a) and 4 (b)]. The forward (backward) coherent rate

$$k_{DA(AD)} = k_{DA(AD)}^{(0)}\mathrm{e}^{-\zeta_{TET}(N-1)}, \tag{56}$$

exhibits an exponential drop with the attenuation coefficient $\zeta_{TET} = \zeta_1 + \zeta_2$ determined by Eq. (44). The pre-exponential factor $k_{DA(AD)}^{(0)}$ is the two-electron super-exchange transfer rate through a bridge with a single unit.

3.3. Proton-assisted reduction of mycothione reductase

The enzyme mycothione reductase (MycR ≡ E) demonstrates specific electron-transfer pathways during redox reactions [53, 54]. We consider one of them, associated with two-electron reduction of enzyme by the oxidant nicotinamide adenine dinucleotide phosphate (NADP). Experimental data shows [55] that this reduction is controlled by the protonation/deprotonation of the active site Cys_{34}–S–S–Cys_{39} of enzyme (E ≡ MycR). In the oxidized enzyme E_{ox} the –S–S– group binds the amino acids Cys_{34} and Cys_{39}, while in twofold reduced enzymes $(E_{red}H)^-$ and E_{red}^{2-} the binding between these amino acids is broken. This transforms the active site into the protonated and deprotonated structures [Cys_{34}–S^-, Cys_{39}–SH] and [Cys_{34}–S^-, Cys_{39}–S^-], respectively. Transformation of the oxidized enzyme E_{ox} requires several electron and proton coupled steps. Here, a special role belongs to flavin adenine dinuleotide (FAD), which, having received electrons from NADP, then participates as an electron donor at the final stage of two-electron transfer. The measured rate of the formation of the reduced enzyme E_{red} is $K_{red} = K_{TET} \approx 130\ \mathrm{s}^{-1}$. This indicates that the characteristic time of the two-electron transport under consideration, $\tau_{TET} \sim 10^{-2}$ s, is much greater than the characteristic times of vibrational relaxation (τ_{vib}) and protonation/deprotonation process ($\tau_{pr/dp}$). Let us denote by $P_{s(a)}^{(m)}(t)$ the occupancies of the mth electronic state in the presence of protonated ($s = pr$) or deprotonated ($s = dp$) group a. Due to the inequality

$$\tau_{TET} \gg \tau_{pr/dp}, \tau_{vib} \tag{57}$$

the temporal evolution of the occupancies $P_{s(a)}^{(m)}(t)$ change on the time scale $\Delta t \sim \tau_{TET}$ in the same way as their integral occupancy $P_m(t)$:

$$P_{s(a)}^{(m)}(t) = f_{s(a)}^{(m)} P_m(t),$$

$$P_m(t) = P_{pr(a)}^{(m)}(t) + P_{dp(a)}^{(m)}(t). \tag{58}$$

The weight of the protonation (deprononation) fraction in the mth electronic state is determined by the functions

$$f_{pr(a)}^{(m)} = \frac{1}{1 + 10^{\mathrm{pH} - \mathrm{pK}_a^{(m)}}},$$

$$f_{dp(a)}^{(m)} = \frac{1}{1 + 10^{\mathrm{pK}_a^{(m)} - \mathrm{pH}}}, \tag{59}$$

(we use notations $\mathrm{pH} \equiv -\log_{10}[\mathrm{H}^+]$ and $\mathrm{pK}_a^{(m)} \equiv \equiv -\log_{10} \mathrm{K}_a^{(m)}$, where $[\mathrm{H}^+]$ is the concentration of protons in the environment, and $\mathrm{K}_a^{(m)}$ is a constant characterizing the binding of a proton to the a group of the system in the mth state). In the example under consideration, the first step of two-electron transfer is the binding of NADP to FAD–E_{ox} and the formation of the charged fraction

$NADP^+$–$FADH^-$–E_{ox}, which is affected by the protonation/deprotonation of the group with pK ≃ 9.1. This group is supposed to be Arg, so the weight of the formed fraction is proportional to $f^{(ox)}_{pr(Arg)}$. Fixing only the main formed fractions of the complex NADP–FAD–E, we can assume that the two-electron reduction of E include the departure of one electron from $NADP^+$–$FADH^-$–E_{ox} (≡ D) and the formation of intermediate fraction $NADP^+$–FAD^{*-}–EH(≡ I). After this, the transfer of the second electron occurs with the formation of the final two-fold reduced deprotonated fraction $NADP^+$–FAD–E^{2-}_{red} (≡ A(*dp*)). This sequential pathway D→I→A is characterized by the rate $k^{(step)}_{TET}$, Eq. (54). The gap $E_I - E_{D(A)}$ between the intermediate and donor (acceptor) states exceeds several k_BT. This leads to the inequalities $k^{(1)}_f \ll k^{(1)}_b$ and $k^{(2)}_f \gg k^{(2)}_b$. If additionally $k^{(2)}_f \gg k^{(1)}_b$, then $k^{(step)}_{TET} \approx k^{(1)}_f$. This rate is proportional of the weight of the protonated Arg during the formation of a two-electron donor center in the complex $NADP^+$–$FADH^-$–E_{ox}. Therefore,

$$k^{(step)}_{TET} \approx f^{(D)}_{pr(Arg)} k_{D\to I}. \tag{60}$$

The coherent pathway D→A is associated with a one-step two-electron transfer. The corresponding rate $k^{(conc)}_{TET} \approx k_{DA}$, Eq. (55) is formed when the amino acid Arg is protonated with weight $f^{(D)}_{pr(Arg)}$ while the amino acid Cys_{39} is deprotonated with weight $f^{(A)}_{dp(Cys_{39})}$. Thus,

$$k^{(conc)}_{TET} \approx f^{(D)}_{pr(Arg)} f^{(A)}_{dp(Cys_{39})} k_{D\to A}. \tag{61}$$

Rates $k_{D\to I}$ and $k_{D\to A}$ are pH-independent values that can be estimated using quantum-chemical methods. In the semiphenomenological approach, they are considered as fitting parameters. Figure 5 exhibits a bell-shaped behavior of $k_{red} = K_{TET}$ versus pH, which corresponds to the theoretical expression (61) showing a concert (synchronic) mechanism of two-electron reduction.

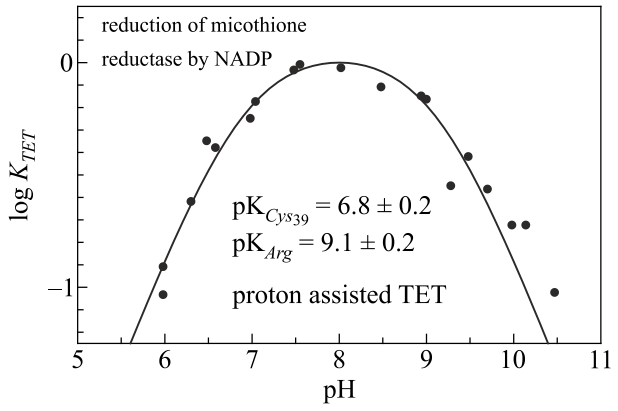

Fig. 5. The bell-shaped pH-dependence of the rate of transfer of two electrons from NADP to enzyme MycR indicates a concert (coherent) transfer mechanism (adapted from [52]).

3.4. Oxygen-mediated transfer of triplet excitations in the pigment-protein complex

Pigment-protein complexes with carotenoid (Car) and chlorophyll (Chl) molecules play a decisive role in photosynthesis, participating in the conversion of light quanta energy into chemical energy. One of the functions of carotenoids in carotinoid-containing photosynthetic proteins is the quenching of triplet excitations of chlorophyll with use of the triplet-triplet energy transfer (TTET) reaction $^3Chl^* + {}^1Car \to {}^1Chl + {}^3Car^*$. This prevents the formation of highly reactive singlet oxygen $^1O^*_2$ resulting from the excitation-transfer reaction $^3Chl^* + {}^3O_2 \to {}^1Chl + {}^1O^*_2$, which is especially effective under aerobic conditions in the absence of carotinoids [56]. In the presence of carotenoids, singlet oxygen is quenched in accordance with reaction $^1O^*_2 + {}^1Car \to {}^3O_2 + {}^3Car^*$.

Direct triplet transfer between Chl and Car molecules can prevent singlet oxygen formation only at rather small, ∼(3–4) Å, distance between these molecules. If it is not the case, then the TTET must be mediated by the bridging unit/units. In certain membrane-bound protein complexes, the role of the bridging unit is often played by the oxygen molecule. Here, we discuss a triplet-triplet transfer between the Chl *a* and Car (β-carotene) in cytochrome b_6f complex. In this complex, a molecular oxygen enters a specific intraprotein channel connecting the Chl *a* and Car [57]. This provides a sufficiently fast triplet-triplet $^3Chl\,a^* \to {}^3Car^*$ excitation transfer and, simultaneously, prevents the formation of the $^1O^*_2$. It is important that both a rather fast quenching of the Chl *a* by the β-carotene and protection against the formation of singlet oxygen are carried out under conditions when β-carotene is about 14 Å from Chl *a*. A possible physical explanation is discussed below based on the model of four electronic states of the complex [Chl *a*, O_2, β-Car]. In their ground electronic states, the Chl *a* and β-Car molecules have zero spin, and in the lowest excited states their spins are equal to 1. In contrast, the O_2 molecule has spins 1 and 0 in its ground and excited states, respectively. We denote by $m_s = 0, \pm 1$ the projections of a spin $S = 1$, and by $l = \pi^*_x, \pi^*_y$ — the atomic orbitals of the O_2 molecule. In complex [Chl *a*, O_2, β-Car], there is no direct coupling between the spaced molecules Chl *a* ≡ *D* and β-Car ≡ *A*, which appear in TTET as a donor and an acceptor of a triplet excitation, respectively. Regarding the coupling of the O_2 mediator with D and A molecules, the magnitude of this coupling is too small to noticeably change the electronic spectra of D and A. Consequently, the O_2–D(A) interaction can be considered as a perturbation and the following expressions can be used for excited initial (I), bridging (B), excited final (F) and ground (G) electronic states of complex [Chl *a*, O_2, β-Car]:

$$|I(m_s)\rangle \simeq |^3D^*(-m_s)\rangle\,|^3O_2(m_s)\rangle\,|^1A\rangle,$$

$$|B(l)\rangle \simeq |^1D\rangle\,|^1O_2^*(l)\rangle\,|^1A\rangle,$$

$$|F(m_s')\rangle \simeq |^1D\rangle\,|^3O_2(m_s')\rangle\,|^3A^*(-m_s')\rangle$$

$$|G(m_s')\rangle \simeq |^1D\rangle\,|^3O_2(m_s')\rangle\,|^1A\rangle. \qquad (62)$$

Since TETT is considered in the absence of the magnetic field, the degeneracy with respect to the spin projection is not removed, and thus the energies of the above states are independent of m_S and l:

$$\mathcal{E}_I \simeq E(^3D^*) + E(^3O_2) + E(^1A),$$

$$\mathcal{E}_B \simeq E(^1D) + E(^1O_2^*) + E(^1A),$$

$$\mathcal{E}_F \simeq E(^1D) + E(^3O_2) + E(^3A^*),$$

$$\mathcal{E}_G \simeq E(^1D) + E(^3O_2) + E(^1A). \qquad (63)$$

Considering complex [Chl a, O_2, β-Car] as an open system, we arrive at kinetic equations (17), where, due to the presence of degeneracy, the role of m is played by $I(m_s)$, $B(l)$, $F(m_s')$ and $G(m_s')$. Taking into account the fact that degeneracy is conserved during triplet energy transfer, we can analyze this transfer using the integral occupancies

$$P_J(t) = \sum_{m_s=0,\pm1} P_{J(m_s)}(t),\ (J = I, F, G),$$

$$P_B(t) = \sum_{l=\pi_x^*,\pi_y^*} P_{B(l)}(t). \qquad (64)$$

The temporal behavior of these occupancies is governed by kinetic equations (17), where the transfer rates are [58]

$$K_{BI(F)} = 3K_{O_2D(A)} \equiv r_{i(f)},$$

$$K_{IF(FI)} = 3K_{D(A)A(D)} \equiv r_{if(fi)},$$

$$K_{I(F)B} = 2K_{D(A)O_2} \equiv r_{-i(-f)}. \qquad (65)$$

Here, elementary backward and forward rates are determined by equations (19) and (20) as well as the relations

$$K_{D(A)O_2} = K_{O_2D(A)} e^{-\Delta\mathcal{E}_{D(A)}/k_BT},$$

$$K_{AD} = K_{DA} e^{-\Delta\mathcal{E}/k_BT}, \qquad (66)$$

where $\Delta\mathcal{E}_{D(A)} \simeq \mathcal{E}_B - \mathcal{E}_{I(F)}$ (cf. Fig. 6) and $\Delta\mathcal{E} \simeq \mathcal{E}_I - \mathcal{E}_F$ are the gap controlling the TTET.

The characteristic time of the TTET in the b_6f complex is $\tau_{TTET} < 8$ ns [57] while the characteristic excitation decay times τ_{dec} for the $^3Chl^*a \to {}^1Chl\,a$, $^3Car^* \to {}^1Car$, and $^1O_2^* \to {}^3O_2$ transitions are (100–400) μs, (1–5) μs and 20 μs, respectively. As

$$\tau_{TTET} \ll \tau_{dec}, \qquad (67)$$

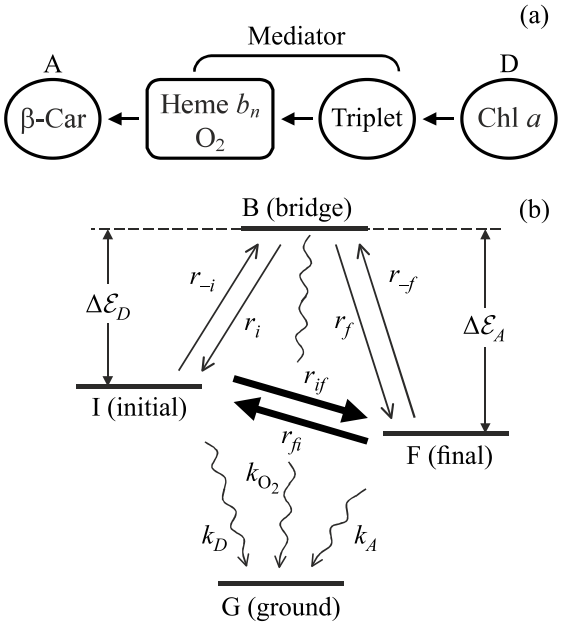

Fig. 6. A possible way of transferring two triplet excitations from Chl a to β-Car through the mediator structure in the pigment-protein complex b_6f (a) and scheme of the transfer of triplet excitation from the initial state I = $^3Chl^{*3}O_2{}^1Car$ to the final F = $^1Chl^3O_2{}^3Car^*$ with the participation of the bridge state B = $^1Chl^1O_2^*{}^1Car$ (b). Degradation of excitation brings the complex to the ground state G = $^1Chl^3O_2{}^1Car$ (b).

there are two different characteristic time scales for the transfer of excitations. This allows us to represent the temporary behavior of the occupancies of excited states as

$$P_J(t) \simeq P_J^{(tr)}(t)P(t). \qquad (68)$$

Occupancies $P_J^{(tr)}(t)$ evolve on the time scale $\Delta t \sim \tau_{TTET}$ and are characterized by the transfer rates (65), (cf. the scheme in Fig. 6). If we replace $r_{-i(-f)} \to k_f^{(1(2))}$, $r_{i(f)} \to k_b^{(1(2))}$ and $r_{if(fi)} \to k_{DA(AD)}$, then matematically the expression for $P_J^{(tr)}(t)$ becomes of the same form as the expression defined by the Eq. (50). The overall transfer rates K_1 and K_2 are given by Eq. (47) where now

$$c_1 = r_f + r_{-f} + r_{fi}, \quad c_2 = r_{if} - r_f,$$

$$d_1 = r_i + r_{-i} + r_{if}, \quad d_2 = r_{fi} - r_i. \qquad (69)$$

These quantities determine the two-exponential regime of TTET via the excitation transfer rates (65) and (66). Despite the fact that molecular oxygen in the b_6f complex facilitates the transfer of triplet excitation from Chl a to β-Car, nevertheless, the formation of reactive singlet oxygen $^1O_2^*$ was not detected in this complex. Within the framework of the physical model under consideration, this means a negligible probability $P_B(t)$ of the formation of bridge state B($^1Chl\,^1O_2^*\,^1Car$) mediating the TTET [cf. Fig. 6(b)]. The structure of complex b_6f is such that an oxygen molecule fixed near heme b_n is noticeably closer to β-Car than to Chl a, Fig. 6(a).

Therefore, the emptying of the state $|B\rangle$ due to the process B→A occurs much faster than the filling of the $|B\rangle$ due to the process I→B. As a result, the fraction of toxic oxygen $^1O_2^*$ is practically not formed (Fig. 7), and TTET looks like a jump of triplet excitation from Chl *a*(D) to β-Car(A), occurring at a rate

$$K_{TTET} \simeq K_2 = K_{D\to A}(1+\mathrm{e}^{-\Delta\mathcal{E}/k_BT}). \tag{70}$$

Forward TTET rate

$$K_{D\to A} = r_{if}^{(\mathrm{seq})} + r_{if} \tag{71}$$

contains contributions $r_{if}^{(\mathrm{seq})} = r_{-i}r_f/(r_i+r_f)$ and r_{if} associated with sequential and coherent routes, respectively. Which route is preferred depends largely on the sign of the gap $\Delta\mathcal{E}_D = E_B - E_I$, which in accordance with the Eq. (63) corresponds to the difference $\Delta E_{O_2}(^1\Delta_g \to {}^3\Sigma_g^-) - -\Delta E_{\mathrm{Chl}\,a}(S_0 \to T)$ between energies of singlet-triplet excitations for Chl *a* and O_2 molecules. If $\Delta\mathcal{E}_D > 0$, then the involving of the sequential route in the TTET requires temperature activation, whereas the coherent route can work even at low temperature. Qualitative estimations show [58] that the sign of the gap $\Delta\mathcal{E}_D$ can be positive or negative dependently on the polarity of the groups surrounding the complex [Chl *a*, O_2, β-Car]. Therefore, to clarify the pathways of transfer of triplet excitation from Chl *a*, to β-Car in the pigment-protein complex b_6f, experimental data are needed to describe the kinetics of transfer on a time scale of 0.1–1 ns. The possible kinetics of such transport is shown in Fig. 7.

The TTET is carried out by converting two triplet excitations (TT) into two singlet (SS) excitations (I→B transition) and two singlet excitations into two triplet ones (B→F transition), Fig. 6(b). Since there is no direct contact between mediator O and pigments Chl *a* and β-Car, the TT→SS and SS→TT transitions occurs due to superexchange two-electron coupling between the oxygen molecule and each

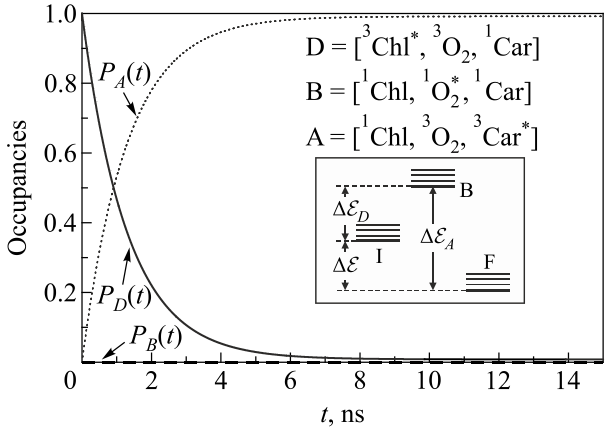

Fig. 7. Kinetics of the triplet transfer in the complex looks like a transfer between donor (Chl) and acceptor (Car), that is, between I and F states only. This is due to the insignificant probability of population of the bridge state, in which singlet oxygen is formed (adapted from [58]).

pigment. Presumably, these couplings are formed with the participation of specific mediators [heme B and tryptophan, Fig. 6(a)]. Estimates show [58] that taking into account these mediators allows one to obtain fairly realistic kinetics characterizing the TTET process in the b_6f complex on the time scale $\Delta t \sim \tau_{TTET} = K_{TTET}^{-1}$, see also Fig. 7:

$$P_D^{(\mathrm{tr})} = \frac{1}{K_1K_2}(r_ir_{fi} + r_fr_{fi} + r_ir_{-f}),$$

$$P_{O_2}^{(\mathrm{tr})} = \frac{1}{K_1K_2}(r_{-i}r_{fi} + r_{-i}r_{-f} + r_{if}r_{-f}),$$

$$P_A^{(\mathrm{tr})} = \frac{1}{K_1K_2}(r_ir_{if} + r_fr_{if} + r_fr_{-i}). \tag{72}$$

These values can be considered as the initial occupancies for the slow process of degradation of the excited states of the complex. To find the corresponding characteristic decay time τ_{dec}, we substitute $P_J^{(\mathrm{tr})}$ into the Eq. (68). If the inequality (67) is satisfied, then taking into account the normalization condition $P(t) + P_G(t) = 1$ and the fact that $\dot P_G(t) = -\sum_J k_J \dot P_J(t) = -\sum_J k_J P_J^{(\mathrm{tr})} \dot P(t)$, we obtain

$$P_G(t) = 1 - \mathrm{e}^{-k_{\mathrm{dec}}t}. \tag{73}$$

Thus, the characteristic decay time $\tau_{\mathrm{dec}} = k_{\mathrm{dec}}^{-1}$ is expressed through the rate

$$k_{\mathrm{dec}} = P_D^{(\mathrm{tr})}k_D + P_{O_2}^{(\mathrm{tr})}k_{O_2} + P_A^{(\mathrm{tr})}k_A, \tag{74}$$

which characterizes the decay of excitation in the complex [Chl *a*, O_2, β-Car]. With a small quasi-stationary occupation of the initial I and bridging B states of the pigment-protein complex, the decay is mainly associated with the $^3\mathrm{Car}^* \to {}^1\mathrm{Car}$ transition in the β-Car pigment. In this case, $k_{\mathrm{dec}} \simeq k_A$.

3.5. Unique temperature-independent transitions

Temperature independent transitions are usually associated with quantum tunneling processes. As applied to biological systems, the tunneling was recorded in the 60s when considering the electron transfer from a high-potential cytochrome to an oxidized dimer of chlorophyll [59]. The explanation and description of this process was carried out within the framework of the theory of donor-acceptor electron transport [15] (the basic formulae of the theory follow from the Eqs. (19) and (20) for m, m' = D, A). However, in biosystems, temperature-independent reactions not associated with the processes of photosynthesis were also revealed. Here we discuss the desentization of ATP $P2X_3$ receptors [60], which takes place in a physiologically important region.

The $P2X_3$ receptors belong to the family of ionotropic receptors widely evolved in the peripherical nervous system. These receptors bind ATP molecules to specific gates of the selective transmembrane ion pores. The gates can be in the open (op) or closed (cl) conformations. It has been shown

experimentally (cf. Fig. 8) that different ATP-induced selective ionic currents $I(t)$ manifest themselves as the same (almost identical) two-stage decrease. The corresponding temporal behavior of the probability of receptor desensitization, $P_d(t) = 1 - I(t)/I_0$, looks like [60]

$$P_d(t) = 1 - [A\mathrm{e}^{-t/\tau_1} + (1-A)\mathrm{e}^{-t/\tau_2}] \qquad (75)$$

with parameters $A \simeq 0.97$, $\tau_1 = 14.7$ ms and $\tau_2 = 230$ ms characterizing the pre-exponential weight and the two temperature-independent decay constants, respectively. To understand the physics of such unique temperature-independent behavior, we will follow the approach that takes into account the role of thermodynamic fluctuations in the formation of transitions between states of an open system. The description can be done on the basis of a kinetic approach using balance equations (17), where the transition rates are evaluated with Eq. (19).

A model is used in which the channel can be in only two physiologically important states (open and closed) [11, 60, 61]. In this case, the simplest explanation of the two-exponential temporal behavior of desensitization is achieved if two types of channels, $j = 1, 2$, are responsible for desensitization.The current through the N_j channels of the jth type, $I_j(t) = N_j i_j P_{\mathrm{op}}^{(j)}(t)$, is determined by the current i_j through an open separate channel and the probability $P_{\mathrm{op}}^{(j)}(t)$ that the channel is open. Since $I(t) = \sum_j I_j(t)$, we get $I(t)/I(0) = AP_{\mathrm{op}}^{(1)}(t) + (1-A)P_{\mathrm{op}}^{(2)}(t)$ where $A = N_1 i_1/(N_1 i_1 + N_2 i_2)$. To determine the temporal behavior of probabilities $P_{\mathrm{op}}^{(j)}(t)$, we assume that transitions between the states $m(s) = \mathrm{op}(s)$ and $m'(s') = \mathrm{cl}(s')$, are quasi-isoenergetic, but the states are degenerate in the number of

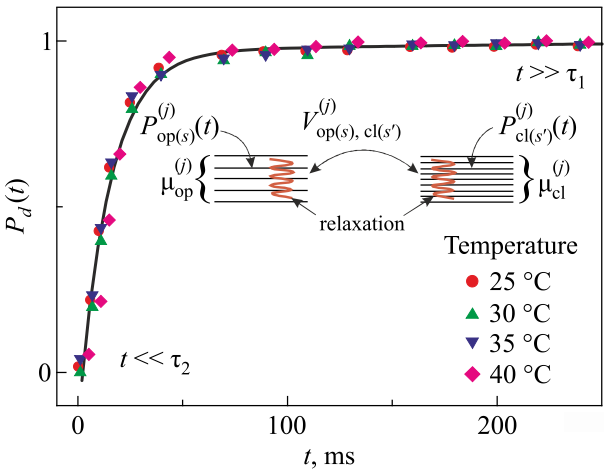

Fig. 8. Temperature-independent two-exponential kinetics corresponding to the onset of desensitization of $P2X_3$ receptor (adapted from [61]). The direction of the desensitization reaction is due to the nonrecurrent kinetics, when the degeneracy $\mu_{\mathrm{cl}}^{(j)}$ of the closed state of the channel is much higher than the degeneracy $\mu_{\mathrm{op}}^{(j)}$ of its open state.

conformational substates $s = 1, 2, \ldots, \mu_{\mathrm{op}}^{(j)}$ and $s' = 1, 2, \ldots, \mu_{\mathrm{cl}}^{(j)}$. Then, according to expression (19), the equation describing the temporal behavior of the occupation of sth substate of the state op reads

$$\dot{P}_{\mathrm{op}(s)}^{(j)}(t) = -\sum_{s'=1}^{\mu_{\mathrm{cl}}^{(j)}} \left[K_{\mathrm{op}(s)\mathrm{cl}(s')}^{(j)} P_{\mathrm{op}(s)}^{(j)}(t) - K_{\mathrm{cl}(s')\mathrm{op}(s)}^{(j)} P_{\mathrm{cl}(s')}^{(j)}(t) \right]. \qquad (76)$$

Transitions between substates $s(s')$ belonging to the state open (closed) occur for the corresponding characteristic times $\tau_{\mathrm{op}}^{(j)}(\tau_{\mathrm{cl}}^{(j)})$, which are much less than the characteristic times $\tau_j \sim (10-100)$ ms of the transition process $\mathrm{op} \to \mathrm{cl}$. Therefore, the substate occupancy is defined as $P_{m(s)}^{(j)} = (1/\mu_m^{(j)}) P_m^{(j)}(t)$ where $P_m^{(j)}(t) = \sum_{s=1}^{\mu_m^{(j)}} P_{m(s)}^{(j)}$ is the integral occupancy. Using this relation, we arrive at the equation $\dot{P}_{\mathrm{op}}^{(j)}(t) = -(\mu_{\mathrm{op}}^{(j)})^{-1} K_j P_{\mathrm{op}}^{(j)}(t) + (\mu_{\mathrm{cl}}^{(j)})^{-1} K_j P_{\mathrm{cl}}^{(j)}(t)$ where $K_j = \sum_{ss'} K_{\mathrm{op}(s)\mathrm{cl}(s')}^{(j)} \approx \sum_{ss'} K_{\mathrm{cl}(s')\mathrm{op}(s)}^{(j)}$. Taking the normalization condition $P_{\mathrm{cl}}^{(j)}(t) + P_{\mathrm{op}}^{(j)}(t) = 1$ into account leads to the solution $P_{\mathrm{op}}^{(j)}(t) = [\mu_{\mathrm{cl}}^{(j)}/(\mu_{\mathrm{op}}^{(j)} + \mu_{\mathrm{cl}}^{(j)})]\mathrm{e}^{-k_{\mathrm{tr}}^{(j)} t} + \mu_{\mathrm{op}}^{(j)}/(\mu_{\mathrm{op}}^{(j)} + \mu_{\mathrm{cl}}^{(j)})$ describing a decrease in the integral occupancy with the overall rate $k_{\mathrm{tr}}^{(j)} = [(\mu_{\mathrm{op}}^{(j)} + \mu_{\mathrm{cl}}^{(j)})/\mu_{\mathrm{op}}^{(j)}\mu_{\mathrm{cl}}^{(j)}]K_j$. It is seen that if the degeneracy of the closed state significantly exceeds the degeneracy of the open state, then $P_{\mathrm{op}}^{(j)}(t) \simeq \mathrm{e}^{-k_{\mathrm{tr}}^{(j)} t}$. This is the result of nonrecurrent kinetics, that leads us to the expression (75) where $\tau_{1,2} = [k_{\mathrm{tr}}^{(1,2)}]^{-1}$ and $k_{\mathrm{tr}}^{(j)} \simeq (\mu_{\mathrm{op}}^{(j)})^{-1} K_j$.

Calculation of the transition rate K_j is based on expressions (19) and (12). We formally put $m = \mathrm{op}(s)$, $m' = \mathrm{cl}(s')$ and estimate the $K_{mm'}^{(j)}$ using the one-phonon approximation, in which $\Lambda_{m'm}(\tau) = \sum_\lambda |M_{m'm}^{(\lambda)}|^2 [(\bar{n}_\lambda + 1)\mathrm{e}^{i\omega_\lambda \tau} + \bar{n}_\lambda \mathrm{e}^{-i\omega_\lambda \tau}]$. Here, $M_{m'm}^{(\lambda)} = \chi_{mm'}^{(\lambda)}$ is the matrix element of the transition between adiabatic terms m and m'. The transition is accompanied by absorption or emission of a phonon of frequency ω_λ, Eq. (10). If a one-phonon transition occurs between the nonadiabatic terms, then $M_{mm'}^{(\lambda)} = V_{mm'} g_{mm'}^{(\lambda)}$, where $V_{mm'} = V_{\mathrm{op}(s),\mathrm{cl}(s')}^{(j)}$ is the matrix element of transition between the substates of diabatic terms (cf. Eq. (9) and inset in Fig. 8). If random deviations of the energy difference $E_m - E_{m'}$ are caused by the thermodynamic fluctuations of the vibration energy $\sum_\lambda \hbar\omega_\lambda (n_\lambda + 1/2)$, then in the classical and quantum limits the factor $F_{mm'}(\tau)$ is given by Eqs. (30) and (31), respectively. Substituting the above expressions for $\Lambda_{m'm}(\tau)$ and $F_{mm'}(\tau)$ into the integral of expression (19) we obtain

$$K_j = \sum_{ss'} K_{mm'}^{(j)} = \frac{1}{\hbar^2} \sum_{ss'} \sum_{\lambda} |M_{mm'}^{(\lambda)}|^2 \times$$

$$\times \sum_{\xi=1,2} \left\{ \frac{(\bar{n}_\lambda + 1)\gamma_\lambda}{\gamma_\lambda^2 + [\Omega_{mm'} - \omega_\lambda + (-1)^\xi \sigma_\lambda]^2} + \right.$$

$$\left. + \frac{\bar{n}_\lambda \gamma_\lambda}{\gamma_\lambda^2 + [\Omega_{mm'} + \omega_\lambda + (-1)^\xi \sigma_\lambda]^2} \right\}, \qquad (77)$$

where $\gamma_\lambda = \gamma_{\text{stoch}}$. If among the set of modes λ there are modes $\lambda = \lambda_*$, the connection with which leads to the appearance of resonance at $\Omega_{mm'} = \pm\omega_* + (-1)^\xi \sigma_*$, then the main contribution to the rate K_j will be made by the resonance terms like $(\bar{n}_* + 1)/\gamma_*$ and $\bar{n}_*/\gamma_*$. According to the expression (30), we have $\gamma_* \sim k_B T$. As $\bar{n}_* + 1 \approx \bar{n}_* \simeq k_B T/\hbar\omega_\lambda$, we see that $(\bar{n}_* + 1)/\gamma_*$ and $\bar{n}_*/\gamma_*$ are independent of temperature. Therefore, the rates K_j and thus, the degradation times $\tau_j = \mu_{\text{op}}^{(j)} K_j^{-1}$ are also temperature-independent characteristics of the process of desensitization.

3.6. Conformational regulation of enzymatic reactions

Enzymes are natural nanocatalysts. Nowadays it is generally recognized that the unique peculiarities of their functioning are attributed to not only their active center specificity but also structural changeability of the whole macromolecule. In this subsection we briefly trace the role of this distinctive property of biomacromolecules in regulatory mechanisms of enzymatic reactions. In the reactions of the enzyme (E) with the substrate (S), the probabilities of the free ($P_E(t)$) and bound (P_{ES_j}) states of the enzyme change while maintaining the normalization condition

$$\sum_j P_j(t) = 1 \quad (j = E, ES_1, ES_2, \ldots). \qquad (78)$$

In enzymatic reactions, the total concentration of enzyme, $[E_t]$, does not change. Therefore, the condition (78) is identical to equality $[E_t] = [E] + \sum_j [ES_j]$, where $[E]$ and $[ES_j]$ are the concentrations of the free enzyme and the complex "enzyme+substrate" in the jth state, respectively. In traditional enzymology, concentrations are used instead of corresponding probabilities $P_E = [E]/[E_t]$ and $P_{ES_j} = [ES_j]/[E_t]$ to describe the reactions of an enzyme with a substrate.

The basis of enzymology is represented by celebrated Michaelis–Menten's scheme. Introduced more than a century ago [62], it still serves as a starting point of any experimental or theoretical investigation in the field. According to this scheme, a reaction of converting substrate S into product P via formation of complex ES with enzyme-catalyst E is described within simple chemical kinetics based on the mass action law as

$$E + S \underset{k_b}{\overset{k}{\rightleftharpoons}} ES \xrightarrow{k_c} E + P,$$

$$d[ES]/dt = -(k_b + k_c)[ES] + k[S][E], \qquad (79)$$

where $[S]$ is the substrate concentration. From Eq. (79), the famous expression for the stationary reaction velocity $v = d[P]/dt = k_c[E_t][S]/([S] + K_M)$ immediately follows (here K_M is Michaelis' constant, $K_M = (k_b + k_c)/k$, and $[E_t] = [E] + [ES]$ is the total enzyme concentration). For a long time, the hyperbolic dependence $v([S])$ served as a validity test of investigation of any enzyme, and deviations from it were considered as artefacts. The situation began changing in the second part of the last century, when the problem of regulation/control of enzymatic reactions gradually became central [63]. In the first place, it concerned revisions of the mentioned hyperbolic dependence in favor of rather trigger-like ones, with considerable velocity differences in narrower substrate concentration intervals. For this, in the first models of cooperativity, apart from allostery (the presence of several binding sites in an oligomeric biomolecule), different conformations of the reaction states have been necessarily introduced [64].

Later, it turned out that "cooperativity" (in the sense of sigmoid dependences on [S]) could be exhibited even by non-allosteric enzymes with an only binding site [65, 66]. For a prolonged period, this elegant idea based in fact on protein structured memory was beyond the enzymology mainstream and provoked a vivid interest only recently (mostly caused by experimental confirmations of the effect in some enzymatic reactions of vital physiological importance [67]), up to introducing a special term "allokairy" [68]. Revisions and extensions of the Michaelis–Menten scheme were revived since the beginning of the present century, especially because of implementation of the single-molecule (SM) methods into enzymology. The latter, however, have not brought fundamental changes in theoretical approaches to describing the regulatory role of structural changeability, as either ensemble or SM reactions were (and still are) mainly considered within the standard chemical kinetics schemes, often reduced to sets of linear equations for concentrations or population probabilities of reaction states, respectively. Below we describe the generic models and effects within this traditional framework and then discuss an advanced approach based on the concept of molecular self-organization. The typical phenomena of conformational regulation can be seen even in reactions of monomeric enzymes possessing an only binding site.

3.6.1. Conformational regulation in discrete schemes

The simplest and traditional way to take into account the enzyme structural complexity implies introduction of several conformational (sub)states of a free enzyme and/or enzyme-substrate complex, with conformational transitions between them. For such schemes (which in fact correspond

to the splitting of the Michaelis–Menten scheme into several conformational channels of the reaction) they use the mentioned rate equations. For ensemble reactions, especially for calculating their steady-state velocities, even the stationary solutions are often informative enough. Not much more complex is the case of SM reactions. As it can be concluded from numerous works exploiting this approach, the characteristic effects of conformational regulation show up even under splitting into only two channels; their larger numbers lead to more cumbersome expressions only, adding no truly new mechanisms. The generic minimal schemes of regulation [69, 70] related to nontrivial dependence of the reaction velocity on substrate concentration or unbinding rates are pictured in Fig. 9 (it is sufficient to show the enzyme states only). Scheme in Fig. 9(a) was proposed in [71]. It illustrates a striking effect of reaction acceleration with rate k_b of "unproductive" substrate unbinding growing in a certain initial interval (this possibility was pointed out quite recently [72]). Here Eq. (79) should be obviously replaced by the set

$$\frac{d[ES_1]}{dt} = -(k_b + k_C)[ES_1] + k[S][E],$$

$$\frac{d[ES_2]}{dt} = -(k_b + k_c)[ES_2] + k[S][E] \qquad (80)$$

which, together with the total enzyme concentration conservation condition $[E_t] = [E] + [ES_1] + [ES_2]$, leads to the following stationary reaction velocity:

$$v = \frac{k[S][E_t]\left[k_b(k_C + k_c) + 2k_C k_c\right]}{k[S](2k_b + k_C + k_c) + (k_b + k_c)(k_b + k_C)}. \qquad (81)$$

If the catalytic rates are of similar magnitude, $k_c \approx k_C$, then $v(k_b)$ monotonically decreases, as it is customary for the Michaelis–Menten scheme. If, however, the channels are markedly different in their catalytic rates, $k_C \gg k_c$, then there exist an interval of $v(k_b)$ growing. The effect becomes possible at substrate concentrations satisfying the condition $k[S] > k_c k_C (k_C + k_c)/(k_C - k_c)^2$. This unexpected result can be nevertheless explained rather simply. Indeed, without the possibility of escape from the "deadlock" state ES_2 with too long waiting times of the catalytic stage (thereby without a chance of a new start and subsequent catalysis via state ES_1), the enzyme would be captured in this less functional state. In fact, scheme in Fig. 9(a) represents a particular case of a more general effect of decrease of the mean first passage time in random walks with resetting [73, 74].

Scheme in Fig. 9(b) is a simplified version of Rabin's scheme of "kinetic cooperativity" [63, 65] and uncovers important physical reasons of this distinctive deviation from the classical hyperbolic dependence. Unlike to the previous scheme, here different conformations of the free enzyme with different binding rates, $k > k'$, are introduced. It is assumed that "more active" state E_2 can slowly relax to "less active" state E_1. The higher substrate concentration, the longer the residence time in more active state.

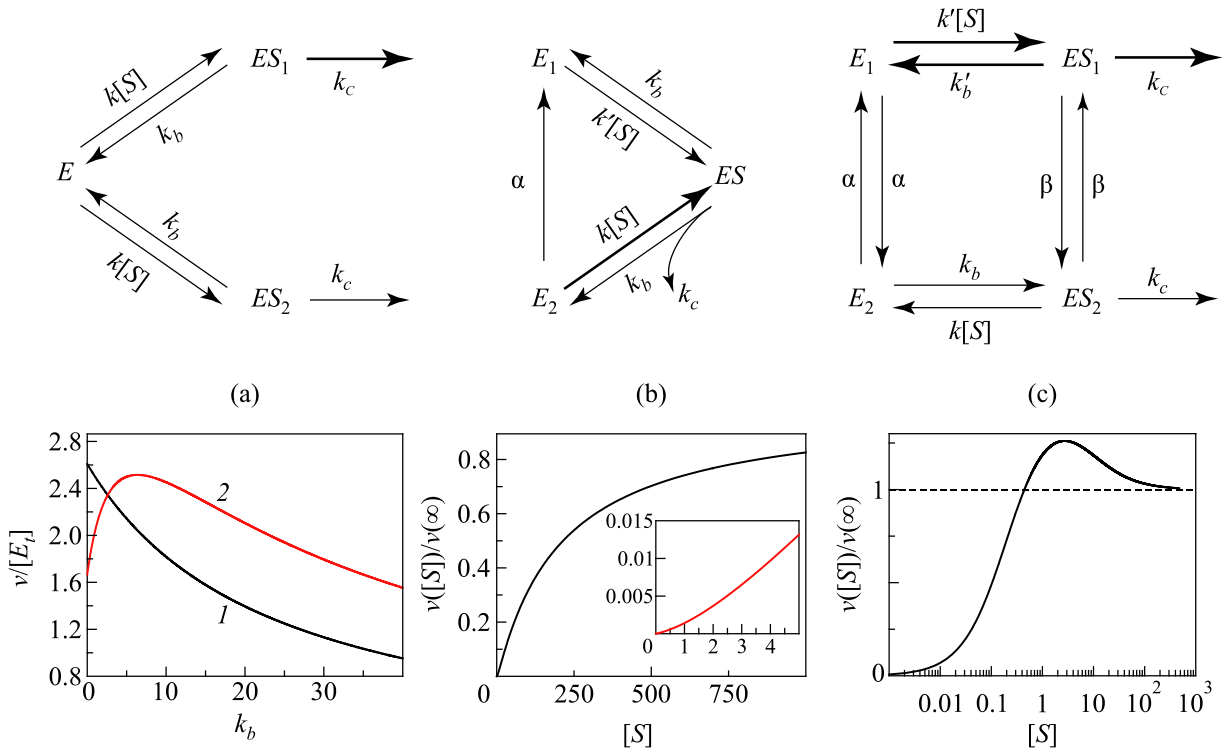

Fig. 9. Reaction schemes and corresponding velocity plots. Plot (a): $k[S] = 10$. $k_C = k_c = 3$ (curve *1*); $k_C = 10$, $k_c = 1$ (curve *2*). Plot (b): $\alpha = 1$, $k = 1$, $k' = 0.1$, $k_b = 10$, $k_c = 100$. Inset: the initial part of the plot for small $[S]$ (see the text). Plot (c): $\alpha = 10$, $\beta = 1$, $k = 1$, $k' = 10$, $b = 10$, $B = 1$, $k_c = 1$, $k_C = 10$.

Under the condition $\alpha < (k_b + k_c)[(k/k') - 1]$ this results in a sigmoid dependence $v([S])$ ("cooperativity") [75]. Various extensions of this scheme are frequently used (see e.g., [67, 68, 76]). It should be noted, however, that in the case of small number of conformation channels the sigmoid behavior is barely seen (as in Fig. 9(b) where it is slightly discernible in the inset only). This is common for linear schemes of discrete conformations, classical schemes of cooperativity included — in the latter, the more macromolecule subunits, the more pronounced cooperativity.

Finally, scheme in Fig. 9(c) admits, in addition to the effects described above, the possibility of self-inhibition (again, in the case of markedly different catalytic rates). Under certain condition on the system parameters (see [69] for details), the role of the less active channel can prevail with $[S]$ growing, and the reaction velocity decreases, see the plot in Fig. 9(c).

With these three effects, the non-standard deviations from classical Michaelis–Menten's theory, related to conformational regulation, are seemingly exhausted. Generalizations towards more complex discrete schemes (e.g., [76]) lead to very bulky expressions while hardly producing new meaningful physical insight.

Almost all recent works in the field concern reactions of single enzymes, since this experimental technique is becoming dominant. It allows one to observe enzyme functioning in a serial regime of consecutive conversions of substrates into products, one by one, and to obtain arrays of turnover times and their probability density $f(t)$. The reciprocal $\langle t\rangle^{-1}$ of the mean turnover time $\langle t\rangle = \int_0^\infty tf(t)dt$ (in fact, mean first passage time [74]) plays the part of the reaction velocity while the higher moments $\langle t^m\rangle$ reflect "dynamical disorder", *etc*. For theoretical derivations of $f(t)$, the same discrete schemes are used with the only difference that the kinetic equations are formulated for probabilities $P_E(t), P_{ES}(t)$ of the reaction system residence in corresponding states. It should be noted, however, that the problem becomes non-stationary (the stage of the enzyme return into the initial free state is not taken into account). Correspondingly, the conservation condition (78) does not hold true any longer, and attempts to preserve it (e.g., [77, 78]) lead to unnecessary inconsistence only.

It is easy to show that $\langle t\rangle^{-1}$ calculated for classical Michaelis–Menten's scheme (79) in such a way is equal to $k[S]/([S]+K_M)$, that is $\langle t\rangle^{-1} = v/[E_t]$. This important relationship, connecting the ensemble and SM results, was called "single molecule Michaelis–Menten equation" and verified experimentally [77, 79]. Remarkably, it remains valid in the presence of conformational splitting of the reaction pathway as well [69]. Thus, being interested in the reaction velocity, it is sufficient to calculate it in the stationary cases of ensemble schemes, which is much simpler. For example, calculation of $v/[E_t]$ performed in [69] for the ensemble version of scheme in Fig. 9(c) has resulted in the expression identical to that obtained for $\langle t\rangle^{-1}$ in a much more laborious way.

3.6.2. Conformational regulation as an example of molecular self-organization

All the schemes discussed above imply essentially non-equilibrium flow conditions (the part of the flow intensity is played by substrate concentration $[S]$). This provokes one to speculate about possible synergetic mechanisms of conformational regulation. According to Haken [80], the necessary conditions of self-organization phenomena include, apart from the flow, a pronounced temporal hierarchy and nonlinearity of the system dynamics. These conditions are practically omnipresent in biomolecular processes, enzyme functioning included. The spectrum of biomolecule structural movements is very broad and includes, in particular, those much slower ones than elementary acts and turnovers of the reaction. Due to such structural memory, cumulative structural changes caused by consecutive substrate arrivals become possible. In turn, these changes entail changes in reaction rates, and this feedback ensures nonlinearity in the system. As a result, stationary non-equilibrium regimes of the enzyme functioning emerge which are self-consistent with the flow. Intensity of the latter plays a role of a control parameter, with its changes causing bifurcation phenomena like bistability, that is, emergence/disappearance and coexistence of functional regimes with markedly different reaction velocities, *etc*.

Far from being exotic, these quite natural ideas form the basis of our concept of molecular self-organization [75] which was applied to describing the conformational regulation effects in primary reactions of photosynthesis (see e.g., [81, 82] and references therein). Application of this concept to enzyme functioning is given in [83]. It is supposed that slow structural changes can be represented by a continuous generalized structural coordinate x which the reaction rates become dependent on. The motion along this coordinate is certainly classical and governed, apart from the influence of standard thermal white noise F_L of Langevin's type, by the switching between structural potentials $V_E(x)$, $V_{ES}(x)$ in the corresponding enzyme states. In other words, the substrate arrivals/departures are the source of a specific dichotomous noise F_t [84, 85], with its space of states $\{f_E, f_{ES}\} = \{-dV_E/dx, -dV_{ES}/dx\}$ and characteristics (reaction rates) dependent itself on the structural variable. Thus, the stochastic equation for x reads $\dot{x} = F_t + F_L$, while the master equation for the dichotomous noise is

$$\dot{\rho}_E(t|x) = -k(x)\rho_E(t|x) + [k_b(x) + k_c(x)]\rho_{ES}(t|x),$$
$$\rho_E(t|x) + \rho_{ES}(t|x) = 1,$$

where ρ_E, ρ_{ES} are the probability densities of realization of forces f_E, f_{ES}, respectively. Then it can be shown [84, 85] that the Michaelis–Menten scheme (79) can be

represented by the following evolution equations for probability densities $P_E(x,t)$, $P_{ES}(x,t)$:

$$\frac{\partial P_E}{\partial t} = D_E \frac{\partial}{\partial x}\left(\frac{dV_E}{dx} + \frac{\partial}{\partial x}\right)P_E - k(x)P_E + [k_b(x) + k_c(x)]P_{ES},$$

$$\frac{\partial P_{ES}}{\partial t} = D_{ES} \frac{\partial}{\partial x}\left(\frac{dV_{ES}}{dx} + \frac{\partial}{\partial x}\right)P_{ES} + k(x)P_E - [k_b(x) + k_c(x)]P_{ES}, \tag{82}$$

where D_E, D_{ES} stand for the coefficients of diffusion generated by the thermal noise. Eqs.(82) can be considerably simplified by applying the adiabatic approximation, obviously valid due to the slowness of structural movements. Then one arrives at Fokker–Planck's equation for distribution $P(x,t) = P_E(x,t) + P_{ES}(x,t)$ with the following derivative of effective nonequilibrium potential $V^{\text{eff}}(x)$:

$$\frac{dV^{\text{eff}}}{dx} = \frac{dV_E}{dx} + \left(\frac{dV_{ES}}{dx} - \frac{dV_E}{dx}\right)\frac{[S]}{[S] + K_M(x)}. \tag{83}$$

To derive Eq. (83), it was supposed that k is non-distributed, $k = k_1[S]$ (this usually holds in enzyme reaction studies) while Michaelis constant became x-dependent, $K_M(x) = [k_b + k_c]/k_1$. A remarkable property of $V^{\text{eff}}(x)$ is its dependence on flow intensity $[S]$. Thus, if potentials $V_E(x)$, $V_{ES}(x)$ are of a one-well shape, then, with $[S]$ growing, the shape of $V^{\text{eff}}(x)$, gradually transforming from that of $V_E(x)$ to that of $V_{ES}(x)$, may become two-well in some interval of $[S]$. In [83] this is shown for the case when the dependence of Michaelis' constant on x can be reduced to exponential one, $K_M(x) \approx \mathrm{e}^{-x}$ (while the part of generalized structural variable x is played by the affinity that changes due to cumulative actions of substrates). The corresponding emergence of stationary distribution $P_{\text{st}}(x)$ bimodality means the appearance of bistability, that is, coexistence of two enzyme functioning regimes with markedly different reaction velocities. With the strength of substrate-conformation interaction (difference in the positions of minima of $V_E(x)$, $V_{ES}(x)$) exceeding some critical value, the dependence $v([S])$ acquires a pronounced sigmoid shape (see Fig. 10), imitating the cooperativity effect. Also, allowance for realistic dependences $k_c(x)$ leads to the possibility of the self-inhibition effect [83].

The above-described picture of reaction regime regulation represents in fact a fold-type catastrophe in full analogy with non-equilibrium phase transitions of the 1st kind (see [83] for details). As distinct from the typical examples of self-organization occurring in macrosystems, here we have this phenomenon at the level of single molecules.

Experimental confirmations of conformational regulation mechanisms may be rather tricky since the latter are of hidden nature and imply concomitant measurements at very different timescales. For ensemble reactions the corresponding proof is often reduced to a collection of indirect evidences (cf. [81]). In this sense, the new possibilities

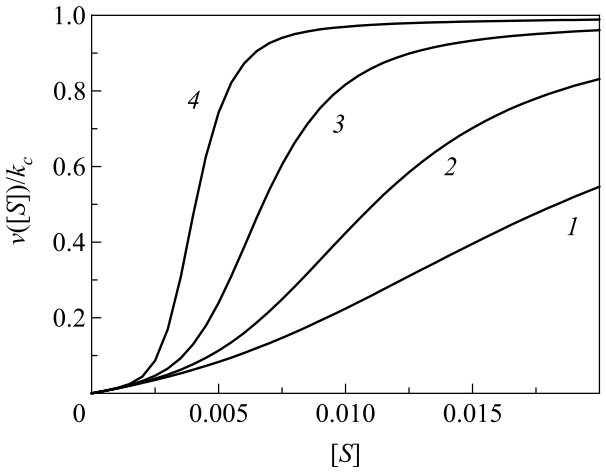

Fig. 10. Dependence $v([S])$ in the self-organization model ($k_c = \text{const}$) [83]. The curves correspond to the strength of substrate-conformation interaction growing from curve 1 to 4.

provided by SM technique look much more promising. To this end, computer simulations of stochastic "SM trajectories" (that is, thousands of turnovers in a model reacting system with realistic parameters which admit bistability) were undertaken in [86]. Their statistical processing has revealed rather eloquent qualitative threshold-like changes in the mean turnover times and behavior of characteristic temporal correlation functions (that is, just in the primary observables in SM experiments) exactly in the bistability area. Detection of such anomalies in scanning a single-enzyme reaction subject to substrate concentration changes would be the most straightforward confirmation of molecular self-organization phenomena at work.

4. Conclusion

The main goal of the work is to show how to describe and analyze the processes of charge/excitation transport and conformational transformations in biosystems under conditions when transport and conformational changes occur against the background of faster processes. Fast processes, such as for example, relaxation among the vibrational levels of electronic terms of biomolecules, stochastic deviation of the energy levels, as well as sorption-desorption of protons, lead to the establishment of a quasi-equilibrium between the probabilities of populating substates and thus facilitate the formation of integral occupancies of molecular terms of the system. Integral occupancies change on a time scale that is much longer than the characteristic times of fast processes occurring between substates. As a result, we obtain averaged kinetic equations that contain the characteristics, which can be estimated from the experiment. This refers also to the equations describing the binding of ligands or substrates to enzymes.

We used the nonequilibrium density matrix method to obtain averaged kinetic equations and indicated criteria for the applicability of these equations to the description of

various types of reactions in biosystems. As an application of the method, we analyzed one-electron and two-electron donor-acceptor transfer between redox centers, as well as the transfer of triplet excitation between pigments in the pigment-protein complex. In both cases, the important role of the bridge structure in the formation of hopping and tunneling (coherent) paths of electron transfer and excitation is shown. The corresponding transfer rates and their dependence on the number of bridging units were found, and for two-electron transfer, the dependence of the rate of the redox reaction on the protonation of amino acids in the enzyme was also estimated. A coarse-grained (averaged) description of transitions between conformationally degenerate states of ion channels made it possible to propose a possible mechanism of channel desensitization.

Within the conventional framework of enzyme kinetics, the generic schemes of conformational regulation of enzymatic reactions are revisited. With the example of a monomeric enzyme with an only binding site, all the possible mechanisms caused by conformational splitting are described for both ensemble or single-enzyme reactions and the simplest ways of calculating the reaction velocity are indicated. An alternative approach based on the ideas of molecular self-organization due to structural memory of the enzyme is outlined.

Acknowlegments

The authors acknowledge support by the National Academy of Sciences of Ukraine, grant “Functional properties of materials perspective for nanotechnologies” (project No. 0120U100858).

1. N. N. Bogoliubov, *Lectures on Quantum Statistics*, Gordon and Breach, New York (1970), Vol. 2.
2. A. I. Akhiezer and S. V. Peletminsky, *Methods of Statistical Physics*, Pergamon Press, Oxford (1981).
3. K. Linderberg and B. J. West, *The Non-equilibrium Statistical Mechanics of Open and Closed Systems*, VCH Publisher, New York (1990).
4. H.-P. Breuer and F. Petruccione, *The Theory of Open Quantum Systems*, Oxford University Press, New York (2002).
5. E. G. Petrov, *Physics of Charge Transfer in Biosystems*, Naukowa Dumka, Kiev (1984).
6. M. Azizi and P. Machnikowski, *Phys. Rev. B* **88**, 115303 (2013).
7. M. del Rey, A. W. Chin, S. F. Huelga, and M. P. Plenio, *J. Phys. Chem. Lett.* **4**, 903 (2013).
8. V. I. Teslenko and E. G. Petrov, *Ukr. J. Phys.* **61**, 627 (2016).
9. E. G. Petrov, Ye. V. Shevchenko, V. I. Teslenko, and V. May, *J. Chem. Phys.* **115**, 7107 (2001).
10. E. G. Petrov, *Bioelectr. Bioenerg.* **48**, 333 (1999).
11. E. G. Petrov and V. I. Teslenko, *Chem. Phys.* **375**, 243 (2010).
12. F. K. Fong, *Theory of Molecular Relaxation*, Wiley, New York (1975).
13. K. Blum, *Density Matrix Theory and Applications*, Plenum Press, New York (1996).
14. V. May and O. Kühn, *Charge and Energy Transfer Dynamics in Molecular Systems*, Wiley-VCH, Weinheim (2004).
15. J. Jortner, *J. Chem. Phys.* **64**, 4860 (1976).
16. R. A. Marcus and N. Sutin, *Biochim. Biophys. Acta* **811**, 265 (1985).
17. E. G. Petrov, V. I. Teslenko, and I. A. Goychuk, *Phys. Rev. E* **49**, 3894 (1994).
18. K. Wodkievicz, B. W. Shore, and J. N. Eberly, *Phys. Rev. A* **30**, 2390 (1984).
19. A. G. Kofman, R. Zeibel, A. M. Levine, and Y. Prior, *Phys. Rev. A* **41**, 6434 (1990).
20. S. Ya. Kilin and A. P. Nozovtsev, *Phys. Rev. A* **42**, 4403 (1990).
21. V. I. Teslenko and O. L. Kapitanchuk, *Int. J. Mod. Phys.* **34**, 2050105 (2020).
22. E. G. Petrov, *Phys. Rev. E* **57**, 94 (1998).
23. T. L. Hill, *Statistical Mechanics*, McGraw-Hill Book Comp., New York (1956).
24. H. Frauenfelder and R. D. Yang, *Mol. Cell Biophys.* **3**, 347 (1986).
25. V. I. Goldansky, Yu. F. Krupyanskii, and V. N. Flerov, *Phys. Scr.* **33**, 527 (1986).
26. E. G. Petrov, *Eur. Phys. J. Special Topics* **216**, 205 (2013).
27. R. Kubo, *J. Math. Phys.* **4**, 174 (1963).
28. N. G. Van Kampen, *Stochastic Processes in Physics and Chemistry*, North-Holland, Amsterdam (1984).
29. V. E. Shapiro and V. M. Loginov, *Physica A* **91**, 563 (1978).
30. A. Brissard and U. Frish, *J. Quant. Spectrosc. Radiat Transfer* **11**, 1767 (1971).
31. A. Brissard and U. Frish, *J. Math. Phys.* **15**, 524 (1974).
32. H. Neuweiler, C. M. Johnson, and A. R. Fersht, *Proc. Natl. Sci. Acad. USA* **106**, 18569 (2009).
33. D. N. Beratan, J. N. Onuchic, and J. J. Hopfield, *J. Chem. Phys.* **86**, 4488 (1987).
34. M. D. Newton, *Chem. Rev.* **91**, 767 (1991).
35. S. S. Isied, M. Y. Ogawa, and J. F. Wishart, *Chem. Rev.* **92**, 381 (1992).
36. B. Giese, J. Amaudrut, A.-K. Köhler, M. Sportman, and S. Wessely, *Nature* **412**, 318 (2001).
37. J. Jortner, M. Bixon, A. A. Voityuk, and N. Rösch, *J. Phys. Chem. A* **106**, 7599 (2002).
38. V. N. Kharkyanen, E. G. Petrov, and I. I. Ukrainskii, *J. Theor. Biol.* **77**, 29 (1978).
39. E. G. Petrov, *Int. J. Quant. Chem.* **16**, 133 (1979).
40. L. N. Christophorov and V. N. Kharkyanen, *Phys. Status Solidi B* **116**, 415 (1983).
41. E. G. Petrov, Ye. V. Shevchenko, and V. May, *Chem. Phys.* **288**, 269 (2003).
42. S. Larsson, *J. Chem. Soc. Faraday Trans. 2: Mol. Chem. Phys.* **79**, 1375 (1983).
43. A. S. Davydov and Yu. B. Gaididei, *Phys. Status Solidi B* **132**, 189 (1995).
44. C. Joachim, *Chem. Phys.* **116**, 339 (1987).
45. J. W. Evenson and M. Karplus, *J. Chem. Phys.* **96**, 5272 (1992).

46. A. Onipko, Y. Klimenko, L. Malysheva, and S. Safström, *Solid State Commun.* **108**, 535 (1998).
47. E. G. Petrov, *Phys. Status Solidi B* **256**, 1900092 (2019).
48. M. G. Ostapenko and E. G. Petrov, *Phys. Status Solidi B* **152**, 239 (1989).
49. A. K. Felts, W. T. Pollard, and R. A. Friesner, *J. Chem, Phys.* **99**, 2929 (1995).
50. D. Segal and A. Nitzan, *Chem. Phys.* **281**, 235 (2002).
51. P. K. Agarwal, S. P. Webb, and S. Hammes-Schiefer, *J. Am. Chem. Soc.* **122**, 4803 (2000).
52. E. G. Petrov, V. I. Teslenko, and V. May, *Phys. Rev. B* **68**, 061916 (2003).
53. E. Ordonez, K. Van Belle, G. Rooss, S. De Galan, M. Letek, J. A. Gil, L. Wyns, L. M. Mateos, and J. Messens, *J. Biol. Chem.* **284**, 15107 (2009).
54. M. Hugo, K. Van Laer, A. M. Reyes, D. Vertommen, J. Messens, R. Radi, and M. Trujillo, *J. Biol. Chem.* **289**, 5228 (2014).
55. A. A. Patel and J. S. Blanchard, *Biochemistry* **40**, 5119 (2001).
56. A. Gall, R. Bereta, M. T. A. Alexandre, A. A. Pascal, L. Burdes, M. M. Mendes-Pinto, S. Andrianambinintsoa, K. V. Stoichkova, A. Marin, L. Valkunas, P. Horton, J. T. M. Kennis, V. van Grondelle, A. Ruban, and D. Robert, *Biophys. J.* **101**, 934 (2011).
57. H. Kim, N. Dashdorj, H. Zhang, J. Yan, W. A. Cramer, and S. Savikhin, *Biophys. J.* **89**, L28, (2005).
58. E. G. Petrov, B. Robert, S. H. Lin, and L. Valkunas, *Biophys. J.* **109**, 1735 (2015).
59. D. De Vault, J. H. Parkes, and B. Chance, *Nature* **215**, 642 (1967).
60. V. Khmyz, O. Maximuk, V. Teslenko, A. Verkhratsky, and O. Krishtal, *Pflüger Arch. Eur. J. Physiol.* **456**, 339 (2008).
61. V. I. Teslenko, E. G. Petrov, A. Verkhradsky, and O. Krishtal, *Phys. Rev. Lett.* **104**, 178105 (2010).
62. L. Michaelis and M. L. Menten, *Biochem. Z.* **49**, 333 (1913).
63. A. Cornish-Bowden, *Perspective in Science* **4**, 3 (2015).
64. J. Monod, J. Wyman, and J.-P. Changeaux, *J. Mol. Biol.* **12**, 88 (1965).
65. B. R. Rabin, *Biochem. J.* **102**, 22c (1967).
66. A. Cornish-Bowden and M. L. Cardenas, *J. Theor. Biol.* **124**, 1 (1987).
67. A. C. Wittington, M. Larion, J. M. Bowler, K. M. Ramsey, B. Bruschweiler, and B. G. Miller, *Proc. Natl. Acad. Sci. USA* **112**, 11553 (2015).
68. V. J. Hilser, J. A. Anderson, and H. N. Motlagh, *Proc. Natl. Acad. Sci. USA* **112**, 11430 (2015).
69. L. N. Christophorov, *Ukr. J. Phys.* **65**, 412 (2020).
70. L. N. Christophorov, *Nanosystems, Nanomaterials, Nanotechnologies* **18**, 541 (2020).
71. L. N. Christophorov, *Dopov. Nac. Akad. Nauk Ukr.* **1**, 40 (2019).
72. S. Reuveni, M. Urbakh, and J. Klafter, *Proc. Natl. Acad. Sci. USA* **111**, 4391 (2014).
73. M. R. Evans and S. N. Majumdar, *Phys. Rev. Lett.* **106**, 160601 (2011).
74. L. N. Christophorov, *J. Phys. A* **54**, 015001 (2021).
75. L. N. Christophorov and V. N. Kharkyanen, *Chem. Phys.* **319**, 330 (2005).
76. J. Wu, D. E. Piephoff, and J. Cao, *J. Phys. Chem. Lett.* **8**, 3619 (2017).
77. S. C. Kou, B. J. Cherayil, W. Min, B. P. English, and X. S. Xie, *J. Phys. Chem. B* **109**, 19068 (2005).
78. A. Kumar, H. Maity, and A. Dua, *J. Phys. Chem. B* **119**, 8490 (2015).
79. B. P. English, W. Min, A. M. van Oijen, K. T. Lee, G. Luo, H. Sun, B. J. Cherayil, S. C. Kou, and X. S. Xie, *Nat. Chem. Biol.* **2**, 87 (2006).
80. H. Haken, *Synergetics, Springer Series in Synergetics,* Springer-Verlag, Berlin, Heidelberg, New York (1978), Vol. 1.
81. Yu. M. Barabash, N. M. Berezetskaya, L. N. Christophorov, A. O. Goushcha, and V. N. Kharkyanen, *J. Chem. Phys.* **116**, 4339 (2002).
82. A. O. Goushcha, A. J. Manzo, G. W. Scott, L. N. Christophorov, P. P. Knox, Yu. M. Barabash, M. T. Kapoustina, N. M. Berezetskaya, and V. N. Kharkyanen, *Biophys. J.* **84**, 1146 (2003).
83. L. N. Christophorov, *AIP Adv.* **8**, 125326 (2018).
84. L. N. Christophorov, *J. Biol. Phys.* **22**, 197 (1996).
85. L. N. Christophorov, A. R. Holzwarth, V. N. Kharkyanen, and F. van Mourik, *Chem. Phys.* **256**, 45 (2000).
86. L. N. Christophorov, V. N. Kharkyanen, and N. M. Berezetskaya, *Chem. Phys. Lett.* **583**, 170 (2013).

Особливості кінетичних та регуляторних процесів у біосистемах

L. N. Christophorov, V. I. Teslenko, E. G. Petrov

Особливістю біологічних систем є їх суттєва структурна неоднорідність. Це проявляється в тому, що процеси, які спостерігаються на наноскопічному рівні, є багатостадійними в часі. Викладено підхід, який дозволяє на основі методів нерівноважної статистичної механіки отримувати кінетичні рівняння, що уможливлюють опис еволюції повільних процесів на тлі більш швидких. До найбільш важливих швидких процесів належать коливальна релаксація в електронному термі та стохастичні відхилення положення електронних енергетичних рівнів системи від їхніх стаціонарних положень. Як приклад показано, яким чином можна описувати кінетику одно- та двоелектронного переносу через білкові ланцюжки, передачу триплетного збудження в пігмент-білковому комплексі за участю кисню, кінетику температурно-незалежної десенсибілізації больових рецепторів, а також конформаційну регуляцію ферментативних реакцій.

Ключові слова: матриця густини, стохастичне поле, релаксація, динаміка конформації.